Vol. 25, No. 19

Mutually Exclusive Subsets of BH3-Only Proteins Are Activated by the p53 and c-Jun N-Terminal Kinase/c-Jun Signaling Pathways during Cortical Neuron Apoptosis Induced by Arsenite

Hon Kit Wong,[1][†][‡] Michael Fricker,[1][†] Andreas Wyttenbach,[1][§] Andreas Villunger,[2] Ewa M. Michalak,[3] Andreas Strasser,[3] and Aviva M. Tolkovsky[1]*

Department of Biochemistry, University of Cambridge, Tennis Court Road, Cambridge CB2 1QW, United Kingdom[1]; Institute of Pathophysiology, University of Innsbruck Medical School, Fritz-Pregl-Str. 3, A-6020 Innsbruck, Austria[2]; and Molecular Genetics of Cancer Division, The Walter and Eliza Hall Institute of Medical Research, Parkville, 3050 Victoria, Australia[3]

The c-Jun N-terminal protein kinase (JNK)/c-Jun and p53 pathways form distinct death-signaling modules in neurons that culminate in Bax-dependent apoptosis. To investigate whether this signaling autonomy is due to recruitment of particular BH3-only proteins, we searched for a toxic signal that would activate both pathways in the same set of neurons. We show that arsenite activates both the JNK/c-Jun and p53 pathways in cortical neurons, which together account for >95% of apoptosis, as determined by using the mixed-lineage kinase (JNK/c-Jun) pathway inhibitor CEP11004 and p53-null mice. Despite the coexistence of both pathways in at least 30% of the population, *Bim* mRNA and protein expression was increased only by the JNK/c-Jun signaling pathway, whereas *Noxa* and *Puma* mRNA and Puma protein expression was entirely JNK/c-Jun independent. About 50% of *Puma/Noxa* expression was p53 dependent, with the remaining signal being independent of both pathways and possibly facilitated by arsenite-induced reduction in P-Akt. However, functionally, Puma was predominant in mediating Bax-dependent apoptosis, as evidenced by the fact that more than 90% of apoptosis was prevented in Puma-null neurons, although Bim was still upregulated, while Bim- and Noxa-null neurons died similarly to wild-type neurons. Thus, the p53 and JNK/c-Jun pathways can activate mutually exclusive subclasses of BH3-only proteins in the same set of neurons. However, other factors besides expression may determine which BH3-only proteins mediate apoptosis.

Proteins of the Bcl-2 family play a crucial role in regulating apoptosis. Of the members that have been shown to have proapoptotic activities, the "BH3-only" clan have been the focus of much attention, as they are highly activated by apoptotic signals (11, 15, 79, 87). While some BH3-only proteins, such as Bid, may chaperone the activation of Bax and Bak at the mitochondrial membrane (11, 36, 87), most others antagonize the functions of the antiapoptotic Bcl-2 family members (13, 80).

In neurons, Bax is a major mediator of apoptosis during development and disease, as many types of neurons that are Bax null are resistant to various apoptotic stimuli (5, 21, 34, 45, 88, 93, 106, 110), though there are exceptions (6, 61). However, though Bax is necessary for neuronal apoptosis (1, 58) through its control of mitochondrial permeability (4), apoptosis by Bax still depends on BH3-only proteins, whose proapoptotic activity, in turn, requires Bax (77). In the central nervous system (CNS), changes in expression of a number of Bcl-2 family members both during development (57) and in model insults,

for example, after axotomy (43, 54, 74, 104), ischemia (81, 91, 114), and kainate-induced seizures (56, 94), have been described. Changes have also been recorded in CNS neurons in culture after various insults, though causal relationships have not always been identified (7, 25, 38, 90, 99). Because most studies have focused on one BH3-only family member, there is currently no consensus as to which proteins are expressed in individual neuron types and little knowledge as to how each of them responds to specific insults at the transcriptional and translational levels. Even one cell type (if not one cell) in the brain may express numerous different Bcl-2 family genes whose composition may change during development (44).

Another key question is which BH3-only proteins are recruited in response to toxic stimuli. In many types of neurons, some death-signaling pathways occur in parallel streams. In particular, the stream triggered by neurotrophic factor withdrawal involves the c-Jun N-terminal kinase (JNK)/c-Jun pathway (9, 38, 39, 78, 107); it is suppressed primarily by phosphatidylinositol 3-kinase (PI3-K)-dependent signals but not by extracellular signal-regulated kinase (ERK)-dependent signals (19, 41, 101, 102, 112). Another stream is a dominant pathway that is mediated by p53 (see, for examples, references 20, 55, 65, 76, 82, 97, 109, 110, and 112). It is suppressed in part by ERK-dependent signals but not by PI3-K-dependent signals (2, 41). Because both pathways are dependent on Bax for apoptosis, it is of great interest to determine at what point the signals converge. We have therefore sought an insult that would trigger both pathways simultaneously but independently.

Arsenite is an environmental toxin that causes multiple developmental and postnatal defects in the CNS (16, 23, 31, 83, 89). When it was fed to rats, numerous areas of the brain showed increased evidence of reactive oxygen species production, in keeping with its known pro-oxidant activity (86). Arsenite has been reported to induce apoptosis in cultured cortical and cerebellar granule neurons through the JNK/c-Jun and p38 pathways (71–73). However, inhibition of these pathways did not result in complete protection from apoptosis. Arsenite has also been shown to cause hyperphosphorylation of tau (33) and to upregulate genes associated with endoplasmic reticulum (ER) stress (68) in cortical neuron cultures, but the signals mediating these responses are not known. In other cell types arsenite is also a potent inducer of the p53 pathway (28, 85, 113), and it can also inhibit survival pathways that play a role in the CNS, such as that mediated by NF-κB (8), by oxidation of a critical cysteine in IκB kinase (49). Because arsenite activates multiple signals, we used it to uncover possible relationships between apoptotic signaling pathways and regulation of Bcl-2 family gene expression.

We demonstrate that arsenite-induced increases in specific BH3-only proteins are signal specific. Bim expression is attenuated by the mixed-lineage kinase (MLK)/JNK/c-Jun pathway inhibitor CEP11004 but is independent of p53. By contrast, Puma and Noxa expression is partially dependent on p53 but is independent of the MLK/JNK/c-Jun pathway. However, there is asymmetry in the impact of these BH3-only proteins on apoptosis, as death is almost entirely prevented in arsenite-treated Puma-null neurons, while there is no significant attenuation of death in Bim- or Noxa-null neurons.

MATERIALS AND METHODS

Materials. Neurobasal medium, B27, SUPERSCRIPT II RNase H⁻ reverse transcriptase, RNAaseOUT, and *Taq* polymerase were from Invitrogen (Paisley, Scotland); papain was from Worthington Biochemical Corp. (Lakewood, NJ); arsenite, cysteine, soybean trypsin inhibitor (STI), propidium iodide (PI), Hoechst 33342, and the bicinchoninic acid protein assay kit were from Sigma (Poole, Dorset, United Kingdom). SP600125 was from Calbiochem (Merck, Nottingham, United Kingdom). All other reagents were from Invitrogen or Sigma. The following antibodies were used: anti-Bad (clone 48), anti-Bcl-2 (clone 7), anti-Bcl-xL/S (clone 4), anti-cytochrome *c* (clone 7H8.2C12), anti-p21 (clone SXM30) (all used at 1:500), anti-ERK1/2 (clone MK12; 1:5,000), and anti-JNK (clone G151-333; 1:1,000) from BD Biosciences (Transduction/Pharmingen), San Diego, CA; anti-P-p53(Ser18) (1:1,000; catalog no. 9284S), anti-P-c-Jun(Ser63) (1:250; catalog no. 9261), anti-P-p38(Thr180/Tyr182) (1:1,000; catalog no. 9211S), and anti-P-JNK(Thr183/Tyr185) (1:1,000; catalog no. 9251) from New England Biolabs; anti-Mdm2 (clone SMP14; 1:500; catalog no. sc965), anti-p53 (FL-393; 1:500; catalog no. sc-6243), and antihemagglutinin (anti-HA) (Y-11; 1:1,000; catalog no. SC 805) from Santa Cruz Biotechnology (Santa Cruz, CA); anti-Bax (clone 5B7; 1:200; catalog no. MS-712-P0) from Neomarkers, Lab Vision (Fremont, CA); anti-Bid (AF860; 1:1,000) from R&D Systems (Minneapolis, MN); anti-Bim (AB17003; 1:1,000) from Chemicon (Temecula, CA); anti-Puma (AB9643; 1:500) from Abcam (Cambridge, United Kingdom); anti-COX(IV) (clone 20E8; 1:500; catalog no. A21348) from Molecular Probes (Eugene, OR); anti-P-S139-H2A.X (1:500; catalog no. 07-164) from Upstate Biotechnology (Lake Placid, NY); and anti-α-tubulin (clone B-5-1-2; 1:5,000; catalog no. T5168) from Sigma (Poole, Dorset, United Kingdom). Anti-p53 (CM5; 1:1,000) was a gift from David Lane (University of Dundee, Dundee, Scotland), and mouse monoclonal anti-P-c-Jun (1 μg/ml) was a gift from Jonathan Ham (ICH, London, United Kingdom). All anti-mouse and anti-rabbit horseradish peroxidase-conjugated and Cy3-conjugated secondary antibodies were from Jackson ImmunoResearch Laboratories (West Grove, PA).

Preparation of cortical neurons from postnatal mice. Cortical neurons were prepared from newborn mice less than 24 h old (129/Ola, CD1, 129/C57BL/6 × CBA background that had been extensively crossed into the CD1 strain, or C57BL/6 strains). Animal use followed Home Office guidelines and approval by Cambridge University's ethical committee. Cerebral hemispheres were minced gently and digested in Neurobasal medium containing papain (20 U/ml) and 0.32 mg/ml L-cysteine for 20 min at 37°C, followed by 20 min at 31°C. Tissues were washed once in Neurobasal medium containing 1 mg/ml bovine serum albumin (BSA) and 1 mg/ml STI, incubated for 2 min at 37°C in Neurobasal medium containing 10 mg/ml BSA and 10 mg/ml STI, washed again in Neurobasal medium, and gently dissociated mechanically with a fire-polished glass pipette. Cells were plated onto poly-L-lysine-coated culture dishes or glass coverslips and maintained in Neurobasal medium containing 1× B27 supplement, 0.5 mM L-glutamine, 100 U/ml penicillin, and 100 μg/ml streptomycin under an atmosphere of 5% CO$_2$–95% air and 100% humidity at 37°C. Cultures were treated on day 6 in vitro (6DIV) and contained about 5% glial fibrillary acidic protein (GFAP)-positive glial cells (determined by scoring numbers of Neu-N- and GFAP-positive cells in two independent cultures). Bax-null mice were a kind gift from Stanley Korsmeyer (Dana-Farber Institute, Boston, MA) and were obtained from Alun Davies (Royal Veterinary College, Edinburgh, Scotland) after extensive crossing into the CD1 background. *Bax* alleles were identified by PCR of genomic DNA purified from tail tips (Bioline, London, United Kingdom) using the following primers: IN5R (5′-TTGACCAGAGTGGCGTAG-3′), EX5F (5′-GCTGATCAGAACCATCATG-3′), and NeoR (5′-GCTTCCATTGCTCAGCG-3′). p53-null mice were a kind gift from Alan Clarke (University of Cardiff, Cardiff, United Kingdom) and were crossed into the CD1 background. *p53* alleles were identified using EX6F (5′-GTGGTGGTACCTTATGAGCC-3′), NeoF (5′-CATCGCCTTCTATCGCCTTC-3′), and IN7R (5′-CAAAGAGCGTTGGGCATGTG-3′). Puma (100)- and Bim (10)-null mice were maintained in a C57BL/6 background. *Puma* alleles were identified using 5′-1 (AGGCTGTCCCTGGGGTCATCCC), 3′-1 (wt) (GGACTGTCGCGGGCTAGACCCTCTG), and 3′-del (ACCGCGGGCTCCGAGTAGC); *Bim* alleles were identified using 5′-1 (PB20) (CATTCTCGTAAGTCCGAGTCT), 3′-1 (PB335) (wt) (GTGCTAACTGAAACCAGA), and 3′-2 (PB65) (mut) (CTCAGTCCATTCATCAACAG).

Quantitation of apoptosis. Apoptosis was quantified by staining with 5 μg/ml PI and Hoechst 33342 to visualize nuclear morphology and distinguish between necrosis and apoptosis. Uniformly blue stained nuclei were scored as healthy, viable cells, while condensed or fragmented nuclei that stained blue were counted as apoptotic. All condensed or fragmented nuclei that stained red were scored as necrotic, even though fragmentation of the nucleus suggests that necrosis is secondary to apoptosis. In cases where only Hoechst 33342 was used, the percentage of fragmented/condensed nuclei is reported. Based on staining of live cultures with PI, about 5% of the neurons were necrotic in untreated 6DIV neuronal cultures. Drugs were added 30 min before stimulation with arsenite.

RT-PCR. RNA was extracted from cortical neurons using the RNeasy Mini kit (QIAGEN, Crawley, West Sussex, United Kingdom) according to the instruction manual and was dissolved in RNase-free water. Total RNA was quantified, and 0.5 μg of RNA from each sample was used for the reverse transcription (RT) reaction. RNA was mixed with 5 μM random hexamers, and the mixture was heated to 70°C for 10 min, after which 1× first-strand buffer, 10 mM dithiothreitol, 0.5 mM deoxynucleoside triphosphates, and 0.75 U RNAaseOUT were added. After incubation at room temperature for 10 min and at 42°C for 2 min, 20 U of SUPERSCRIPT II was added and the reaction mixture was further incubated at 42°C for 50 min and 70°C for 15 min. The PCR mixture contained 0.4 μM forward and reverse target gene primers, 100 nM deoxynucleoside triphosphates, 1.5 mM MgCl$_2$, 1× PCR buffer, and 1.25 U of *Taq* polymerase. Five percent of the cDNA was used for each PCR. The reaction cycle was started by denaturation at 95°C for 10 min, followed by amplification cycles of 1 min each at 95°C, 59°C, and 72°C, with a final extension at 72°C for 10 min. All the primers were 20 nucleotides long with 60% GC content and were designed to amplify 300 to 600 bp (Table 1) so as to have equivalent annealing temperatures and similar amplification efficiencies. The number of amplification cycles used for each primer pair was determined after prior identification of the cycle number that yielded mid-log-phase amplification and was carefully adhered to for each PCR. PCR products were resolved in a 1.5% agarose gel containing 3 μg/ml ethidium bromide by electrophoresis, and band intensities were imaged and quantified with LabWorks analysis software (UVP Products, Cambridge, United Kingdom) after it was determined that band intensities were within the linear range of detection. The intensity values obtained were normalized to the values obtained for glyceraldehyde-3-phosphate dehydrogenase (GAPDH). Primers were designed so that they would hybridize solely within the coding region of mRNA sequences (GenBank database, NCBI) and would span at least two exons. The absence of an amplicon of the appropriate size from genomic DNA was verified for all primers.

Thirteen Bcl-2 family members were expressed in these cultures: four putative

TABLE 1. List of primers for RT-PCR

Gene (product length [bp])	Forward primer	Reverse primer
Bcl-2 (331)	GTCGCTACCGTCGTCACTTC	ACAGCCAGGAGAAATCAAAC
Bcl-w (490)	CGGGCTCTAGTGGCTGACTT	GCACTGTCCTCACTGATGCC
Bcl-xL/xS (560/367)	TAGGACTGAGGCCCCAGAAG	CAGTCATGCCCGTCAGGAAC
Bax (470)	ATCGAGCAGGGAGGATGGCT	CTTCCAGATGGTGAGCGAGG
Bad (494)	GAGGAAGTCCGATCCCGGAA	CGGCGCTTTGTCGCATCTGT
Bid (466)	CCTGCTGGTGTTCGGCTTTC	CGTGTGGAAGACATCACGGA
Bak (297)	ACAGCAGGTTGCCCAGGACA	TGGCCCAACAGAACCACACC
BimEL/L/S (584/416/326)	GGCCAAGCAACCTTCTGATG	GCCTTCTCCATACCAGACGG
Dp5/Hrk (279)	ATGTGCCCGTGTCCCCGGCA	CTACGCGCTCCGCCTGCCGA
Puma/Bbc3 (295)	TCCTCAGCCCTCCCTGTCAC	CCATTTCTGGGGGCTCCAGGA
Noxa (230)	GAACGCGCCAGTGAACCCAA	CTTTGTCTCCAATCCTCCGG
Bok/Mtd (512)	CGGCGCTCTTCTGTCTTTGC	ACATCCGTCCATCCACCACG
Diva (448)	ATTCTTCTGCGCACGGGAGC	TCTTCTCCAGAAGCCGAGCG
Boo (470)	CTAGACGGCTGCTGTCTGAC	TCTCCAGAAGCCGAGCGGTA
Blk (433)	GGCGAGACTTATGGCCAGAG	CAAATACCAGGCCCCACCCA
Bmf (440)	TCTGCTGACCTGTTTGCCCA	TCTTGTCTGTTCAGGGCGAG
GFAP (589)	ACAAGGCGCTGGCAGCTGAA	CTGCAGTTGGCGGCGATAGT
GAPDH (239)	ATTGTCAGCAATGCATCCTG	TTCAGCTCTGGGATGACCTTGCC
p53 (419)	CACAACTGCACAGGGCACCT	CATGGAGGAGTCACAGTCGG

antiapoptotic genes (*Bcl-2*, *Bcl-xL*, *Bcl-w*, *Mcl-1*), two multidomain proapoptotic genes (*Bax*, *Bok/Mtd*), and six BH3-only genes (*Bim*, *Bid*, *Bad*, *Puma*, *Noxa*, *DP5*), as well as *N-Bak*. No transcripts for *Bmf*, *Blk*, *Boo/Diva*, *Bcl-xS*, or full-length *Bak* were detected (data not shown) (108). The contribution of the 5% astrocytes present in the cultures to this profile was found to be negligible: <1% expression was detected when the amount of cDNA derived from pure 6DIV mouse cortical astrocytes was adjusted so that equal amounts of GFAP derived from the cortical neuron cultures and the pure astrocytes were amplified side by side (data not shown) (108). In addition, arsenite did not induce apoptosis in astrocytes, nor was *Noxa* mRNA expression elevated in the astrocytes by 6 μM arsenite over 3 days (data not shown) (108), in contrast with the neurons (see further below).

Subcellular fractionation. Cortical neurons were harvested in phosphate-buffered saline (PBS) and centrifuged at 360 × *g* for 5 min at 20°C. Cell pellets were then resuspended in isotonic buffer (210 mM mannitol, 70 mM sucrose, 1 mM EDTA, and 10 mM HEPES, pH 7.5) supplemented with protease inhibitors (Complete; Roche Diagnostics, Lewes, East Sussex, United Kingdom) and homogenized in a Dounce B homogenizer using 20 strokes. Homogenates were centrifuged at 500 × *g* for 5 min at 4°C, and the supernatant was respun at 500 × *g* for 5 min to remove all the remaining unbroken cells and nuclei. The resulting supernatant was centrifuged at 10,000 × *g* for 30 min at 4°C to obtain the heavy membrane (HM) fraction. The supernatant of this spin was defined as the cytosolic fraction (cyto). In some experiments that used equal volumes of each fraction, the volume of the cytosolic fraction was reduced and concentrated by spinning through a polyethersulfone membrane concentrator (Vivaspin 500; 5,000-molecular-weight cutoff; Vivascience, Epsom, United Kingdom). It should be noted that the total amount of cytosolic proteins per lane (estimated by Ponceau staining) was about fivefold the total amount of HM fraction proteins, causing some background staining.

Immunoblotting. Cultures were rinsed twice with cold PBS before addition of ice-cold lysis buffer at pH 7.4 (containing 8.6% sucrose, 50 mM Tris-Cl, pH 7.4, 1 mM EDTA, 0.038% EGTA, 1% Triton X-100, 1 mM Na₂VO₃, 10 mM NaF, and Complete protease inhibitor cocktail). After 15 min on ice, cells were scraped off and were kept at −80°C. The protein concentration was quantified using a bicinchoninic acid kit, and lysates were then mixed with 4× sodium dodecyl sulfate (SDS) gel-loading buffer to give 30 μg protein per lane (except for fractionation studies). After boiling for 5 min, proteins were resolved in an 8 to 14% polyacrylamide gel and transferred to a nitrocellulose membrane (pore size, 0.22 μm) by electroblotting. The membrane was blocked with 5% low-fat milk (Marvel, Spalding, United Kingdom) in Tris-buffered saline containing 0.1% Triton X-100 for 1 h at room temperature and subsequently incubated with the primary antibody for 1 h at room temperature and/or at 4°C overnight. After a wash, the membrane was incubated with the appropriate horseradish peroxidase-conjugated secondary antibody for 1 h at room temperature and developed by enhanced chemiluminescence using the Amersham Biotech or Promega SuperSignal Femto kit and exposure to Kodak X-Omat film. Films were scanned (HP Scanjet 5470C), and only those values falling within the range of a standard curve were used for quantification.

Viral infection. An adenovirus (Ad) coexpressing HA-Puma and enhanced green fluorescent protein (EGFP) under the control of separate cytomegalovirus (CMV) promoters (115) was kindly provided by J. Yu and B. Vogelstein (HHMI, Baltimore, MD). The virus was propagated in 911 cells, purified on a cesium chloride gradient, and desalted by chromatography on a Sepharose PD-10 column, and aliquots were stored in 10% glycerol at −80°C. Cortical neurons were infected in suspension for 30 min at 37°C at a PFU of 40 before seeding and were fixed after 20 h using 3% paraformaldehyde.

Immunocytochemistry. Cells grown on coverslips were fixed with 3% paraformaldehyde in PBS at room temperature for 20 min, rinsed twice with PBS, and permeabilized in PBS containing 1% BSA and 0.1% saponin at room temperature for 20 min. The primary antibody was diluted in the same buffer and incubated with cells at 4°C overnight. After a wash, the antibody was visualized with Alexa 488- or Cy3-conjugated secondary antibodies and analyzed by confocal microscopy (Olympus IX70 connected to an UltraVIEW LCI confocal imaging system; Perkin-Elmer Life Sciences, Cambridge, United Kingdom).

RESULTS

Postnatal mouse cortical neurons undergo Bax-dependent apoptosis in response to arsenite. Figure 1 shows that 6 μM arsenite induced nuclear fragmentation and condensation (Fig. 1A) after 24 h in 40% of 6DIV neurons and that this effect was completely abrogated by coincubation with 100 μM Boc-Asp(*O*-methyl)-CH₂F (BAF), a pan-caspase inhibitor that shows minimal toxicity in neurons (Fig. 1B). There was no increase in PI-stained neurons above basal values of ~5%, indicating the absence of necrosis (data not shown). Consistent with the findings of Namgung and Xia (73), death induced by arsenite was dependent on macromolecular synthesis, as evidenced by the fact that it was inhibited by coincubation with 1 μg/ml cycloheximide (CHX) or actinomycin D (act-D) (Fig. 1C). Furthermore, arsenite-induced apoptosis was inhibited in neurons derived from the cortices of Bax-null mice (Fig. 1D and E), where survival similar to control values was maintained for at least 3 days. In contrast, all the neurons derived from wild-type (wt) littermate mice (or heterozygotes [not shown]) treated with arsenite died within 3 days.
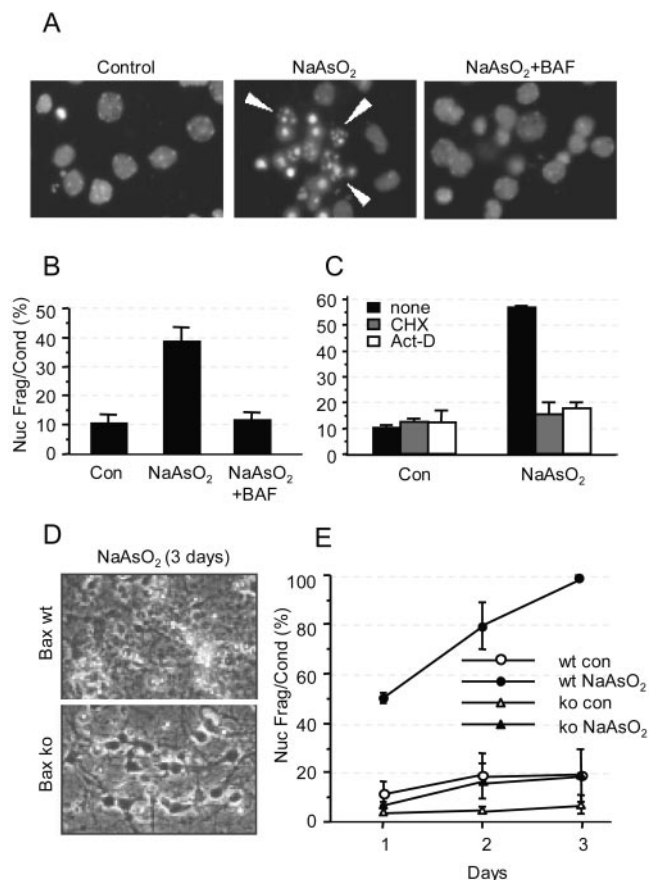
FIG. 1. Arsenite causes Bax- and caspase-dependent apoptosis of mouse cortical neurons that requires macromolecular synthesis. (A) Micrographs showing nuclear morphology of Hoechst 33342-stained 7DIV cortical neurons that were either left untreated (left) or treated with 6 μM arsenite (NaAsO₂) for 24 h (center and right) in the absence (center) or presence (right) of 100 μM BAF. Arrowheads indicate nuclear fragmentation and condensation. (B) Apoptosis was quantified by determining the proportion of neurons containing condensed and fragmented nuclei as indicated in panel A. (C) Cortical neurons were treated with 6 μM arsenite alone (black) or together with 1 μg/ml CHX (gray) or 1 μg/ml act-D (white) for 24 h, after which apoptosis was determined as for panel B. (D) Phase-contrast micrographs showing morphology of wt or Bax-null cortical neurons 3 days after addition of 6 μM arsenite. (E) The percentage of apoptosis was quantified as for panel B. con, control. Error bars, standard errors of the means from three independent experiments.

Bcl-2 family genes respond differentially to arsenite treatment. To identify which members of the Bcl-2 family respond to arsenite at the transcriptional level, neurons were treated with 6 μM arsenite for 20 h, and 100 μM BAF was added to cohort cultures to ensure that the changes observed were not due to destruction of proteins that control synthesis of RNA (22) or protein (12) secondary to caspase activity. Additional cultures were incubated with 1 μg/ml (0.8 μM) act-D, which blocks transcription (at this concentration, incorporation of [³H]uridine into RNA is reduced by 93%), to rule out changes that are due to regulation of mRNA turnover and stability. Figure 2A shows a representative image obtained for each data set for 11 Bcl-2 family gene transcripts compared to *GAPDH* mRNA, used as an internal control, while Fig. 2B shows mean

changes in expression ± 95% confidence intervals based on four to six independent samples. In no case did we find that arsenite altered the stability of the mRNA independently of act-D, nor were there significant differences between the results obtained in the presence or absence of BAF. BAF addition alone also did not alter basal transcript levels (H. Wong, data not shown).

Seven of the genes showed little or no relative change after 20 h of arsenite addition (*N-Bak*, *Bok/Mtd*, *Bcl-2*, *Bax*, *Bcl-xL*, *Bad*, and *Bcl-w*). If anything, the last three transcripts listed displayed a slight (10 to 20%) reduction (range from four independent samples) in steady-state expression. Relative *N-Bak*, *Bok/Mtd*, and *Bcl-w* transcript levels were also largely unaltered during treatment with 1 μg/ml act-D. However, relative *Bcl-2*, *Bax*, *Bcl-xL*, and *Bad* transcript levels were reduced by 50 to 70% (range from four independent samples) after 20 h in the presence of act-D. It is unlikely that act-D itself facilitated gene expression, because transcription of both *p53* and *p21* induced by arsenite was totally inhibited in the presence of 1 μg/ml act-D, though it was induced by noninhibitory concentrations of 5 nM act-D (data not shown) (108), as in other cell types (50).

The second group (*Bim*, *Bid*, *Puma*, and *Noxa*) showed increased relative expression after 20 h of arsenite addition. Transcripts for all three *Bim* splice variants (*-EL*, *-L*, and *-S*) were increased (1.5-, 2.4-, and 2.5-fold, respectively; four to six independent samples), though the relative amounts of *Bim-S* and *Bim-L* mRNAs were about 10- and 3-fold less abundant, respectively, than that of *Bim-EL*. The increase in *Bid* was about 1.3-fold, that of *Puma* was 1.7-fold, and that of *Noxa* was 4-fold (four to six independent samples). Interestingly, *Bim* and *Bid* transcripts showed up to 90% loss of mRNA relative to *GAPDH* over 20 h in the presence of 1 μg/ml act-D, while the higher inducibility of *Puma* and *Noxa* was associated with little apparent loss of transcripts in the presence of 1 μg/ml act-D compared to control cells (four to six independent samples). It is apparent that steady-state levels of mRNA for some transcripts reflect both rates of synthesis and degradation.

Arsenite induces changes in protein expression and localization of Bax, BimEL, and Puma. Although evidence for expression of *Puma* and *Noxa* mRNAs in CNS neurons has been reported recently (18, 47, 53, 81), no studies have been published that examine whether there is coincident expression of Puma, Noxa, and Bim proteins in cortical neurons during apoptosis. We therefore examined how their expression and subcellular distribution are altered by arsenite. For this purpose, arsenite-treated cortical neurons were fractionated into cytosolic and heavy membrane fractions after 12, 18, and 24 h and analyzed by immunoblotting. The $10,000 \times g$ supernatant (cyto) contained ERKs, Akt, and tubulin but no mitochondrial proteins such as ATPβ synthase, while the $10,000 \times g$ pellet (HM) contained no ERKs, Akt, or tubulin but did contain the ER, indicated by the presence of KDEL-containing proteins (data not shown). Because there was protein loss overall in the neurons, especially at the 24-h time point, expression was analyzed by loading equal proportions of cytosolic and HM fractions without correcting for total protein content (Fig. 3A). To follow Puma expression in the HM fraction more quantitatively and to compare its expression to that of cytochrome *c*, a constant amounts (30 μg) of protein from the cytosolic and
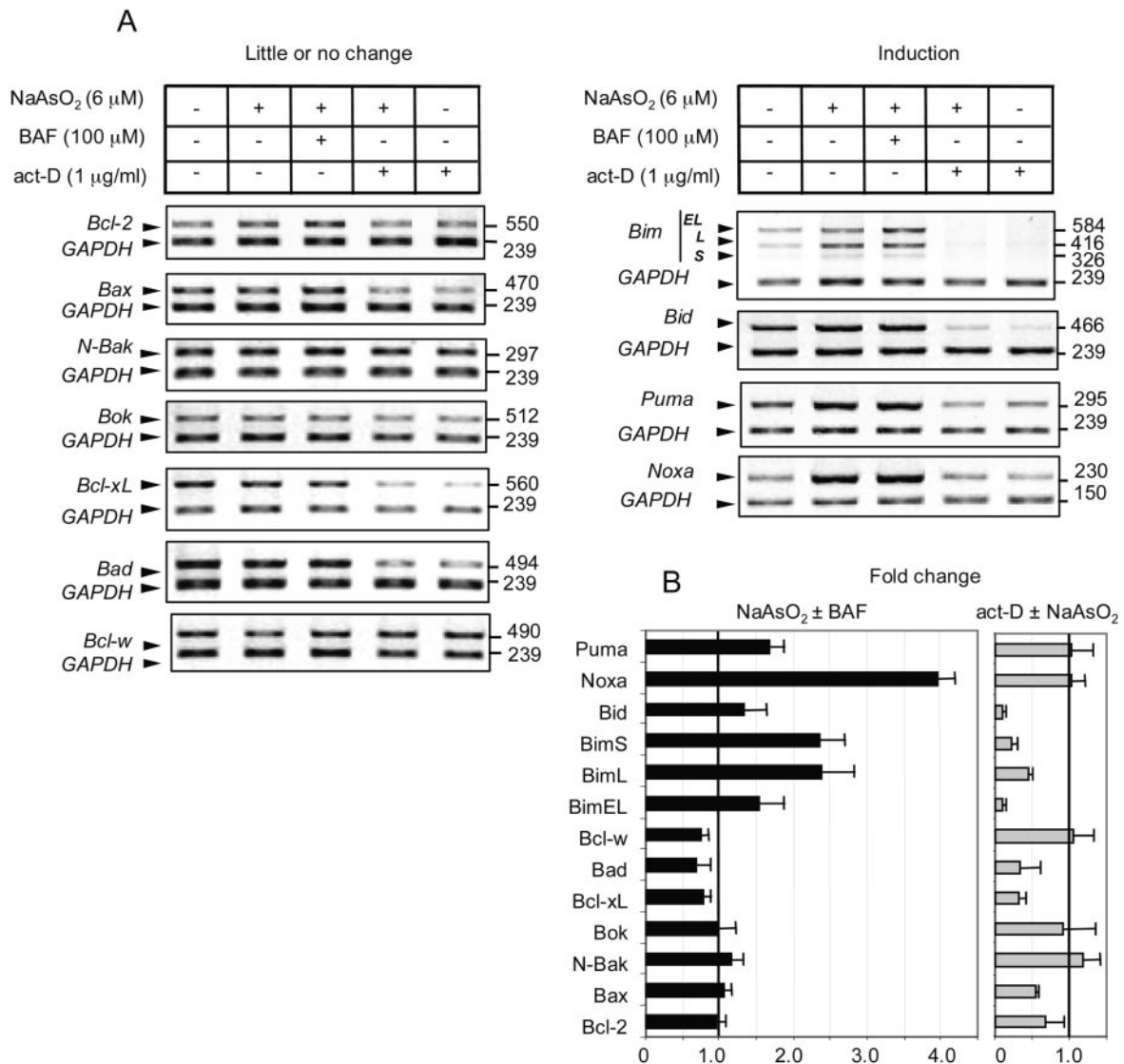
FIG. 2. Arsenite induces *Puma*, *Noxa*, *Bim*, and *Bid* gene expression in 6DIV cortical neurons. (A) Changes in Bcl-2 family gene expression in neurons induced by treatment with 6 μM arsenite in the absence or presence of 100 μM BAF after 20 h, or in the presence of 1 μg/ml act-D (which reduces RNA synthesis by ~93%) alone or with arsenite to investigate mRNA stability. GAPDH was amplified together with each sample as an internal control. Representative panels of ethidium bromide-stained gels after inversion of the digitized image are shown. (B) Mean change in gene expression ± 95% confidence interval from an analysis of four to six replicates. The intensity of each band was normalized to its respective internal control and divided by the normalized value for the untreated control. Error bars show only the upper limit of the 95% confidence interval for clarity, Black bars, change in the presence of arsenite without or with BAF present. Gray bars, change in the presence of act-D without or with arsenite present.

HM fractions was loaded per time point (Fig. 3B). The relative amounts of Puma, Bim (as BimEL, the only form of Bim detected), Bax, and cytochrome *c* in the HM fraction are quantified in Fig. 3C.

Puma expression was almost undetectable in untreated neurons, but it was increased after treatment with arsenite. All of the increase occurred in the HM fraction, consistent with Puma being a mitochondrially targeted protein (70, 116), though its localization to the ER cannot be excluded. The increase was about twofold within 12 h, before there were any signs of apoptosis, and expression remained elevated thereafter ($P < 0.01$ at all time points) (Fig. 3A and B) or even

increased further (see Fig. 7 below). No Puma protein was detected in Puma-null neurons (data not shown). In keeping with the kinetics of apoptosis, the amount of cytochrome *c* in the HM fraction was reduced beginning at 18 h, reaching about 50% of initial values relative to Cox(IV) at 24 h (Fig. 3B). We were unable to detect Noxa using several different antibodies.

In contrast with Puma, there was a considerable amount of BimEL expressed in the untreated neurons, with the HM fraction containing around 60% of total cellular BimEL. This was not a nonspecific band, as no BimEL was detected in Bim-null neurons (Fig. 7B). Arsenite caused an additional small but significant amount (~20%) of cellular BimEL to appear in the
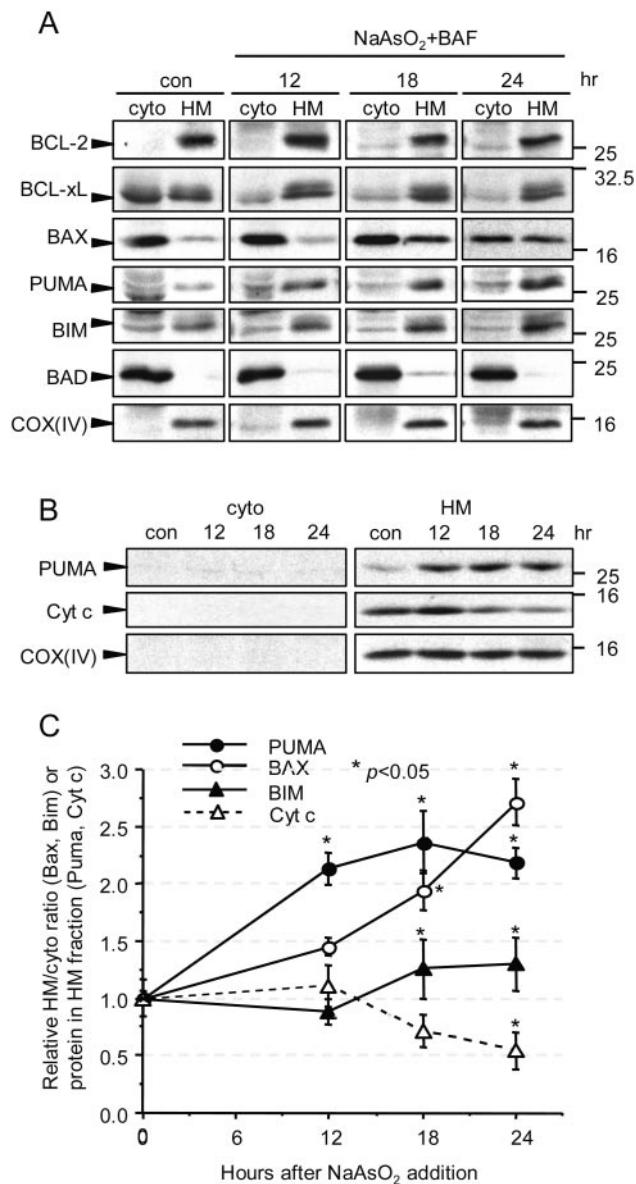
FIG. 3. Amounts of Bax, Bim, and Puma protein are increased in the mitochondrial fraction of neurons after treatment with arsenite. 6DIV cortical neurons were treated with 6 μM arsenite and 100 μM BAF, and lysates were fractionated at the times indicated into an HM fraction and the corresponding cytosol (cyto). Proteins were separated by SDS-polyacrylamide gel electrophoresis and immunoblotted with the indicated antibodies. (A) The same proportion of volume from each cyto and HM fraction was loaded at each time point to assay for protein translocation. In order to match the volume of the HM fraction, the cyto fraction had to be concentrated, causing high background in some of the COX(IV) lanes in the cyto fraction. con, control. (B) A constant amount of protein (30 μg) of the HM and cyto fractions was loaded per lane to compare total amounts of Puma and cytochrome c (Cyt c) in the two fractions. (C) Band intensities of Bax and Bim expressed in the cyto and HM fractions in panel A were measured at each time point, from which the proportion of Bax or Bim in the HM fraction was calculated (mean ± SD from three independent experiments). Since significant amounts of Puma were found only in the HM fraction, band intensities of Puma and cytochrome c expressed in the HM fraction were measured and normalized to those of COX(IV) (mean ± SD from three to four independent experiments). *, $P < 0.05$ for comparison to time zero by Student's t test.

HM fraction within 18 h ($P < 0.05$ at 18 and 24 h), consistent with its proposed role in neuronal apoptosis (78, 107). A 20% increase in BimEL [relative to Cox(IV)] was also measured in the HM fraction at 12, 18, and 24 h when 30 μg of HM protein was loaded per lane, strengthening the evidence for translocation of BimEL.

Bax, too, was significantly enriched in the HM fraction at 18 h (when apoptosis begins to be measurable), and by 24 h about 50% of total cellular Bax was in the HM fraction. However, we could not measure an increase in Bax when 30 μg of HM protein was loaded per lane. In contrast, more than 95% of Bad remained in the cytosolic fraction, and there was little evidence for a change in its expression or localization. We also could not detect any significant increase in Bid protein despite the fact that its mRNA was elevated by 30% and despite the presence of BAF, which prevented loss of Bid due to caspase-mediated Bid cleavage (see data in Fig. 6 below).

Regarding the antiapoptotic family members, Bcl-2 (Fig. 3A) was almost exclusively in the HM fraction, with no significant change in expression or distribution induced by arsenite. Bcl-xL appeared to be distributed equally between the cytosolic and HM fractions in unstimulated neurons, while in arsenite-treated neurons, the amount of Bcl-xL detected in the crude cytosolic fraction declined, consistent with previous observations that it translocates to mitochondria during apoptosis (42, 48). However, although there did not appear to be an enrichment of Bcl-xL in the HM fraction, the total decrease in Bcl-xL did not reach statistical significance. These data show that expression of a select subset of BH3-only proteins increased significantly in response to arsenite without significant changes in overall Bcl-2 and Bcl-xL expression.

The JNK/c-Jun and p53-dependent pathways are the major regulators of arsenite-induced apoptosis. Since *Noxa* and *Puma* expression was increased by arsenite, and both genes were first identified in a screen for p53-dependent proteins, we suspected that p53 might be induced by arsenite in addition to the JNK/c-Jun pathway described previously (73). To address the mechanism of signaling that leads to upregulation of Puma, Noxa (mRNA), and BimEL, we examined whether JNK and its dependent transcription factor c-Jun and/or p53 are activated. We also investigated whether antiapoptotic signals such as those mediated by the PI3-K/Akt pathway (which interacts with and counteracts the JNK pathway [51, 52]) and the ERK pathway (which counteracts the p53 death pathway [2, 41]) were reduced. Figure 4A shows that both P-c-Jun(Ser63) and p53 were increased after treatment with arsenite. The relative amount of P-JNKs—which were already prominent in unstimulated neurons, as reported previously for cortical (73) and other CNS (17, 111) neurons—was not altered (values from seven independent experiments, three conducted without BAF and four conducted with BAF, showed that the phospho-p46 form did not change upon treatment with arsenite [$P = 0.41$ by Student's t test]). However, we did observe a consistent decrease in the minor p54 JNK band (Fig. 4A and 5D).

Since p53 had not been reported to be induced by arsenite in cortical neurons previously, we examined its expression in more detail. Immunocytochemical analysis of p53 expression showed that p53 levels increased in neuronal nuclei in a time-dependent manner (Fig. 4B and C), with about 45% of the nuclei showing intense p53 staining after 24 h. Since p53 stain-
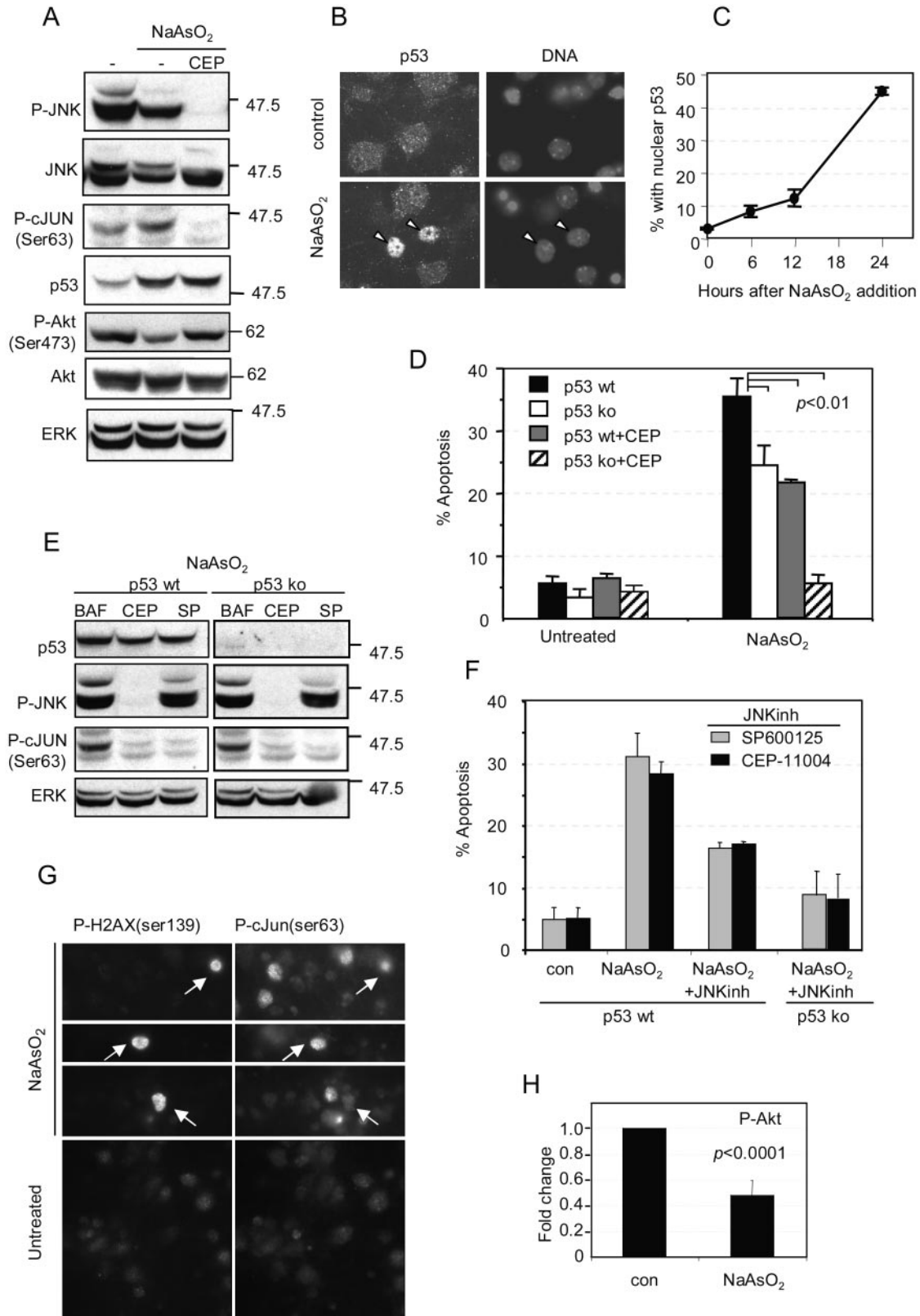
FIG. 4. Arsenite activates c-Jun- and p53-dependent apoptosis and reduces P-Akt(Ser473). (A) 6DIV cortical neurons were treated with 6 μM arsenite for 24 h in the absence (−) or presence (CEP) of 5 μM CEP11004, after which proteins were separated by SDS-polyacrylamide gel electrophoresis and immunoblotted for P-JNK, JNK, P-c-Jun(Ser63), p53, P-Akt(Ser473), Akt, and ERK as a loading control. Note that in the absence of CEP11004, P-c-Jun(Ser63) and p53 expression was increased whereas P-Akt(Ser473) expression was decreased; CEP11004 prevented the phosphorylation of P-JNK and P-c-Jun(Ser63) proteins and the decrease in P-Akt(Ser473) without affecting p53 expression. (B) Neurons were

ing occurred in nonapoptotic neurons, and 80% ± 10% of neurons died between 24 and 48 h, it is clear that p53 was expressed in neurons that went on to die. Commensurate with the increase in p53, p53 became phosphorylated on serine 18 (the equivalent to serine 15 in human p53), p21 mRNA was induced 2.1 ± 0.3-fold, and p21 protein expression increased 10-fold (data not shown) (108). These data suggest that p53 induced by arsenite is transcriptionally active. Regarding the antiapoptotic pathways, the amount of P-Akt(Ser473) was significantly reduced, by 48% ± 10% (Fig. 4H) ($P < 0.0001$ by Student's t test), without any effect on total Akt expression. Interestingly, this effect was not observed within 12 h of arsenite addition. However, there was no change in the amount of P-ERKs, which remained elevated throughout the 24-h cell death period (data not shown) (108). Similar results were obtained when the experiments were performed in the absence or presence of BAF (see, for example, Fig. 6), thus excluding a disproportionate contribution of living (or dead) cells to the data obtained.

To investigate to what extent the p53 and JNK/c-Jun pathways account for arsenite-induced apoptosis within 24 h, we made use of p53-null neurons and the drug CEP11004, an inhibitor of the MLK group of kinases that prevents c-Jun phosphorylation and apoptosis in cortical neurons (29, 32, 69). In the presence of arsenite, CEP11004 (5 μM) completely inhibited JNK phosphorylation up to 24 h and reduced P-c-Jun(Ser63) to below unstimulated levels (Fig. 4A). A similar decrease was found for the amount of total c-Jun (M. Fricker, data not shown), suggesting autoregulation of c-Jun expression by its phosphorylation. In contrast, elevated p53 expression remained sustained and unaltered in the presence of CEP11004, suggesting the lack of interaction between these two signaling pathways. In addition, CEP11004 attenuated the decrease in P-Akt(Ser473) (Fig. 4A).

Figure 4D shows that neurons from p53-null mice were partially resistant to apoptosis induced by arsenite: apoptosis was reduced by 30 to 40% ($P < 0.01$; three independent experiments) compared to apoptosis in neurons from wild-type littermates after 24 h. When CEP11004 was added to neurons derived from wt mice, it also reduced arsenite-induced apoptosis by 30 to 40%. However, together, treatment of p53-null neurons with CEP11004 reduced apoptosis in >95% of the neurons. Virtually identical results were obtained with the JNK inhibitor SP600125 (Fig. 4F) after verification that it—unlike CEP11004—completely abrogated c-Jun phosphorylation

without inhibiting JNK phosphorylation (Fig. 4E). We also investigated whether p38 phosphorylation was activated by arsenite (73), but in keeping with our observation that p38 phosphorylation was delayed until 30 h and so is unlikely to be involved in mediating apoptosis at 24 h, the p38 inhibitor SB203590 (10 μM) did not increase cortical neuron survival significantly after 24 h and CEP11004 did not attenuate phosphorylation of p38 (data not shown) (108).

The data thus far are consistent with the notion that arsenite activates two independent, parallel, and additive death-signaling pathways in cortical neurons, one dominated by JNK/c-Jun signals and one by p53 signals. However, when the percentage of p53-positive nuclei was compared with that of P-c-Jun-(Ser63)-positive nuclei after 20 h, about 80% of the nuclei in the neuron population stained strongly for P-c-Jun(Ser63) while 50% of the population were also strongly stained for p53, at minimum an overlap of 37%. Moreover, a larger overlap (56% ± 8%) was obtained for arsenite-treated neurons after 20 h by costaining with anti-P-H2A.X(Ser139), which identifies double-strand DNA breaks, and anti-P-c-Jun(Ser63) (Fig. 4G). Thus the majority of p53-positive neurons coexpress the JNK/c-Jun(Ser63) pathway, although there are some P-c-Jun-positive neurons that are p53 negative at this time point.

Noxa and *Puma* **mRNA expression and Puma protein expression are dependent on p53 but not on the JNK/c-Jun pathway.** The finding that arsenite induces two independent signaling pathways in the same neurons allowed us to investigate whether the expression of the BH3-only proteins induced by arsenite occurs in a signal-specific manner. When p53 expression was measured side by side with that of Puma in neurons prevented from undergoing apoptosis by use of 100 μM BAF, p53 and Puma expression increased in parallel (Fig. 5A and B). In these experiments, expression of both proteins was elevated about twofold after 12 h, increasing to almost fourfold after 24 h (data not shown). The expression level of both proteins remained high up to 36 h, when almost 70% of the neurons underwent apoptosis (data not shown) (108). Expression of Mdm2, a protein that is induced by p53 and causes p53 destabilization (27, 40, 59, 60), decreased to 20% of initial values between 12 and 24 h (Fig. 5A and B), coincidentally with the further increase in p53. When Puma expression was analyzed in p53-null neurons, the relative expression of *Puma* mRNA (Fig. 5C) and protein (Fig. 5D) induced by arsenite was significantly attenuated, by 48% ± 8%, compared to expression in p53-replete neurons. Reductions were also observed in

---

fixed after 24 h of treatment, immunostained for p53, and visualized using an Alexa 488-conjugated secondary antibody. Nuclei were stained with Hoechst 33342. (C) The percentage of neurons with p53-positive nuclei is shown as a function of time after arsenite addition (mean ± range from two independent experiments). (D) Neurons from p53 wt or p53-null mice were treated with 6 μM arsenite in the absence or presence of 5 μM CEP11004 for 24 h, after which apoptosis was determined in unfixed cultures by scoring the percentage of nuclei stained with Hoechst 33342 that had condensed/fragmented DNA. Nuclei stained with PI were excluded. $P < 0.01$; means ± standard errors of the means from three independent experiments are shown. (E) p53 wt or p53 ko neurons were treated with 6 μM arsenite and either 100 μM BAF, 5 μM CEP11004, or 20 μM SP600125. Note that both the latter compounds blocked c-Jun phosphorylation but only CEP11004 blocked JNK phosphorylation. Neither compound affected p53 expression. (F) Comparison of efficacies of CEP11004 and SP600125. Neurons were treated as for panel D, except that either 5 μM CEP11004 or 20 μM SP600125 was used as a JNK inhibitor (JNKinh). (G) Images of neurons treated with 6 μM arsenite for 20 h, fixed, and costained with an anti-P-H2A.X(Ser139) antibody (with an Alexa 488-conjugated secondary antibody) and an anti-P-c-Jun(Ser63) antibody (with a Cy3-conjugated secondary antibody). Untreated controls were stained side by side. Arrows point to neurons showing costaining for P-c-Jun and P-H2A.X. (H) Reduction in P-Akt(Ser473) in neurons treated with 6 μM arsenite for 24 h. The band intensity of P-Akt was quantified, normalized to total Akt, and divided by the ratio of P-Akt to total Akt in untreated samples after 24 h. Data, from blots similar to those shown in panel A, are means ± standard errors of the means from seven independent experiments.
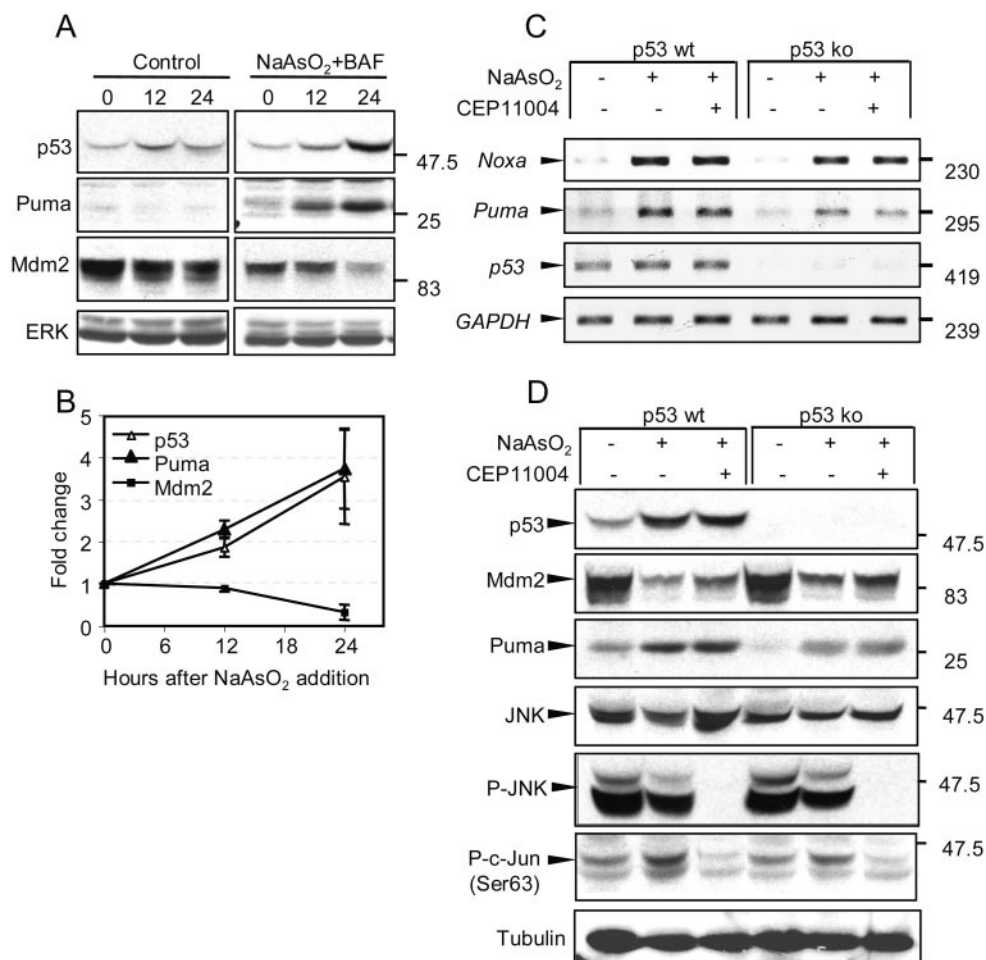
FIG. 5. Induction of *Puma* and *Noxa* mRNA and Puma protein expression is dependent on p53 but is not dependent on the JNK/c-Jun pathway. (A) Neurons were either left untreated (control) or treated with 6 μM arsenite in the presence of 100 μM BAF. Proteins extracted at time zero or after 12 or 24 h were resolved by SDS-polyacrylamide gel electrophoresis, immunoblotted, and probed for p53, Puma, Mdm2, and total ERK as a loading control. (B) Relative amounts of the respective proteins (means ± ranges from two independent experiments). (C) 6DIV neurons from wt or p53-null animals were either left untreated or treated with 6 μM arsenite in the absence or presence of 5 μM CEP11004 for 24 h. *Noxa*, *Puma*, *p53*, and *GAPDH* mRNA expression was detected by RT-PCR. Note the significant decrease in expression of *Puma* and *Noxa* mRNA and the lack of effect of CEP11004 on the inducibility of *Noxa* and *Puma* mRNA. (D) Proteins from neurons treated as for panel A were separated by SDS-polyacrylamide gel electrophoresis and immunoblotted for p53, Mdm2, Puma, JNK, P-JNK, P-c-Jun(Ser63), and tubulin as a loading control. Note that a lack of p53 does not entirely inhibit the induction of Puma expression, though absolute levels are similar to those obtained from untreated p53 wt neurons.

basal levels of *Puma* mRNA and protein in p53-null neurons. However, Puma protein expression in p53-null neurons, and to a lesser extent *Puma* mRNA, was still increased by arsenite, demonstrating that another signaling pathway contributes to its expression. Similarly, the level of *Noxa* transcript expression was also reduced, by 30% ± 5%, compared to that measured in wt neurons, though some expression was still induced in p53-null neurons.

Because CEP11004 inhibited apoptosis in p53-null neurons, we expected that it might be responsible for the residual expression of Puma and Noxa. However, surprisingly, CEP11004 caused no reduction in the amount of Puma protein expression or in *Puma* or *Noxa* gene upregulation irrespective of whether the neurons were from wt or p53-null mice (Fig. 5C and D), although it completely inhibited both JNK and c-Jun phosphorylation induced by arsenite (Fig. 4). A similar lack of

inhibition of Puma/Noxa was obtained with the JNK inhibitor SP600125 (data not shown). Hence, arsenite-induced expression of *Puma* and *Noxa* genes and Puma protein—though partially p53 independent—is independent of the JNK/c-Jun signaling pathway.

Bim expression is under the control of the JNK/c-Jun pathway and is independent of p53. Expression of Bim (primarily BimEL) increases in many types of neurons via a JNK- and c-Jun-dependent pathway (9, 38, 39, 78, 107). However, other transcription factors also contribute to its increased expression (35), but its control by p53 has not been examined. Following treatment with arsenite, BimEL expression rose with kinetics similar to that of P-c-Jun(Ser63), increasing to 2.1 ± 0.3-fold at 12 h (at which time P-c-Jun levels were increased 2 ± 0.5-fold) and declining to 1.5 ± 0.3-fold at 24 h, alongside the reduction of 1.3 ± 0.06-fold in P-c-Jun(Ser63) (errors are standard de-
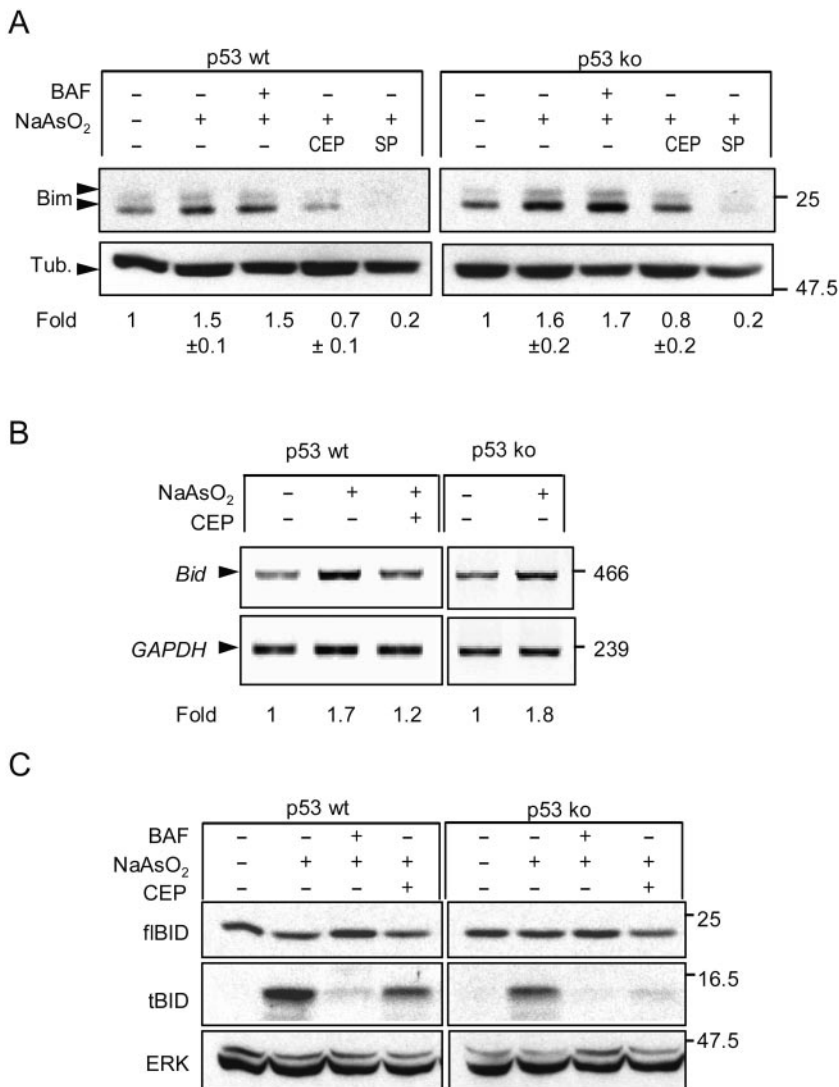
FIG. 6. Induction of Bim and Bid by arsenite is quenched by CEP11004, but induction is not affected by a lack of p53. (A) Cortical neurons from p53 wt or p53-null mice were treated for 24 h with 6 μM arsenite in the absence or presence of 5 μM CEP11004 (CEP) or 20 μM SP600125 (SP). In one sample, 100 μM BAF was added to ensure that survival was at least equivalent to that obtained with CEP. Proteins were extracted, resolved by SDS-polyacrylamide gel electrophoresis, and immunoblotted for Bim and tubulin (Tub.) as a loading control. Note the lack of effect on induction of Bim in p53-null neurons, though basal levels of expression relative to tubulin are higher. (B) Bid mRNA expression analyzed by RT-PCR. Note the suppression of arsenite-induced Bid expression by CEP11004 but the lack of inhibition of arsenite-induced Bid mRNA expression in p53-null neurons. Results of one of two representative experiments for wt neurons are shown. (C) Representative immunoblot (one of three independent experiments) of neurons treated as for panel A except that in addition, 100 μM BAF was added to one of the arsenite-treated cultures. The blot was probed for full length Bid (flBid; exposure, 15 s) and tBid (exposure, 15 min). Note the reduction of flBid in neurons undergoing apoptosis, the prevention of Bid degradation in neurons cotreated with BAF, and the correlation between the amount of reduction in tBid and the amount of apoptosis in the population.

viations [SD] of three independent determinations). In keeping with this correlation, BimEL expression did not increase in neurons cotreated with CEP11004 (Fig. 6A). Furthermore, similar increases in BimEL expression were induced by arsenite in neurons from p53 wt and p53-null mice, while CEP11004 or SP600125 prevented increased BimEL expression in both sets of neurons, demonstrating that arsenite-induced BimEL expression is p53 independent. Thus, it appears that in contrast to that of Puma, BimEL expression induced by arsenite is mediated largely via the MLK/JNK/c-Jun pathway and is not further modulated by p53.

Bid mRNA expression induced by arsenite was also controlled by the JNK/c-Jun pathway and was independent of p53, as evidenced by the fact that expression was attenuated by treatment with CEP11004 to 1.2-fold basal expression, while there was no diminution of expression in p53-null mice (induction in p53 wt and knockout [ko] littermates, 1.7 ± 0.1-fold [range from two experiments] and 1.8-fold, respectively [Fig. 6C]). However, as mentioned above, there was no change in expression of full-length Bid protein. In contrast, in the absence of BAF, we detected a small amount of cleaved Bid (tBid) with a size of 13 kDa, consistent with the size of tBid.
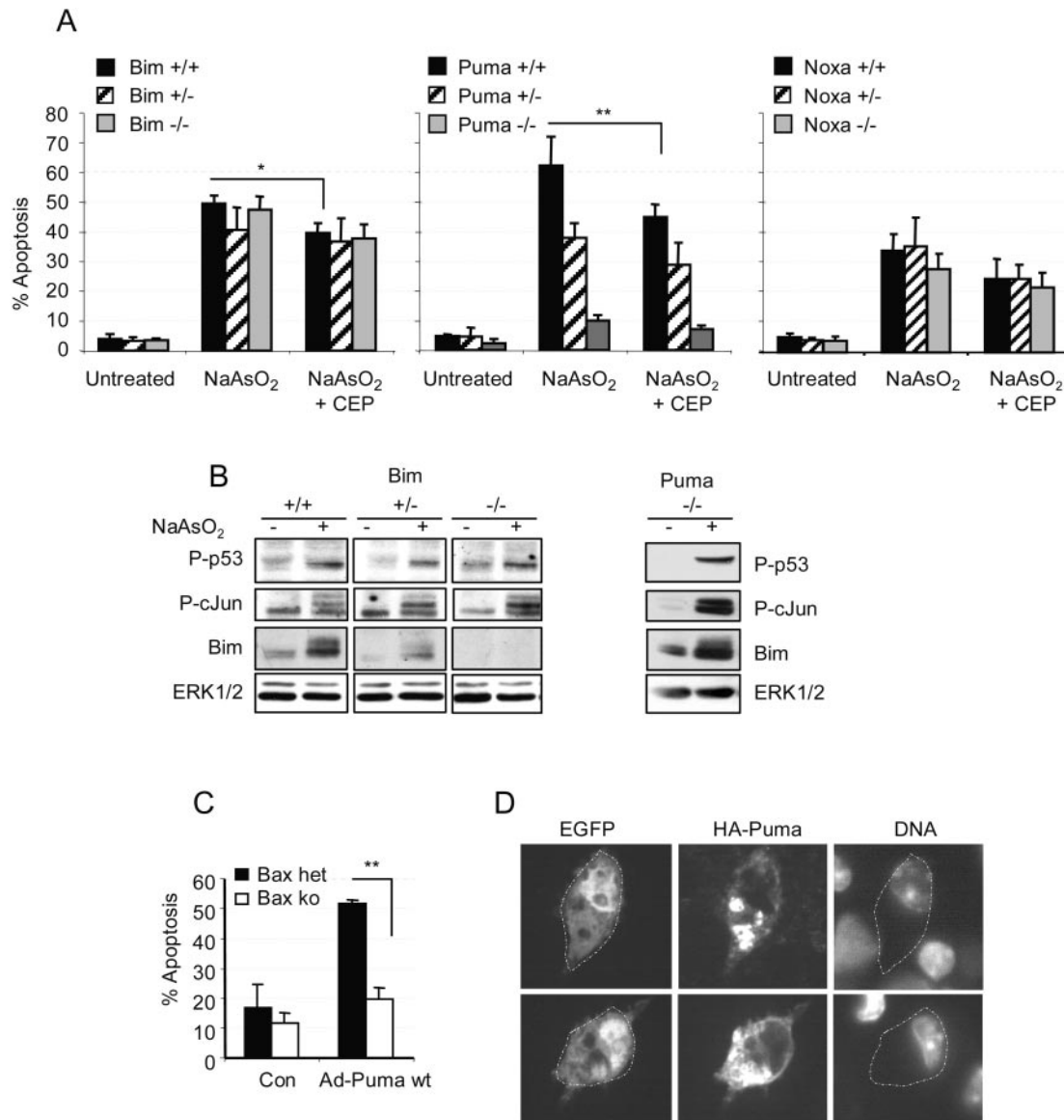
FIG. 7. Puma is the dominant proapoptotic mediator of arsenite-induced, Bax-dependent death. (A) Percent apoptosis of arsenite-treated 6DIV cortical neurons derived from individual cortices of *Bim*, *Puma*, or *Noxa* littermates produced from heterozygote matings (three mice were wt for *Bim*, three for *Puma*, and four for *Noxa*; four mice were heterozygous for *Bim*, five for *Puma*, and four for *Noxa*; there were three *Bim* ko, four *Puma* ko, and four *Noxa* ko mice). Apoptosis was scored after 20 h. Note the lack of inhibition of death in *Bim*- or *Noxa*-null neurons compared to 90% inhibition in *Puma*-null neurons. (B) Blots show that neurons of all three Bim genotypes and of the *Puma* ko genotype express P-p53(Ser18) and P-c-Jun(Ser63), while Bim upregulation (which was 2-fold in wt neurons and 2.1-fold in Puma ko neurons) is *Bim* gene dosage dependent and remains prominent in *Puma* ko neurons. (C) Neurons were cultured from seven animals, four Bax$^{-/-}$ and three Bax$^{+/-}$ cortices. Cultures were infected in suspension with 40 PFU of Ad HA-Puma per neuron, and neurons coexpressing EGFP under the control of a separate CMV promoter in the same construct were scored for apoptosis after 20 h. Control (Con) neurons were uninfected. (D) Images of wt neurons infected with 40 PFU of Ad-Puma per neuron. Neurons were maintained in the presence of 100 µM BAF after infection to prevent apoptosis, fixed after 20 h, and immunostained for HA-Puma using an anti-HA antibody. DNA was stained with Hoechst 33342. Note the punctate localization of HA-Puma in cytoplasmic compartments compared to the diffuse staining of EGFP.

Production of cleaved Bid was inhibited by BAF, indicating that it is a caspase-dependent cleavage product and hence is produced after Bax activation. In keeping with this idea, the amount of tBid produced was proportional to the extent of apoptosis in the population, and its production was completely inhibited in p53-null neurons treated with CEP11004 (Fig. 6C).

Puma—but not Bim—is the predominant mediator of arsenite-induced apoptosis. To establish whether there is a causal relationship between Puma, Bim, and Bax-dependent apoptosis, cortical neurons were prepared from the three genotypes of offspring of Puma-, Bim-, or Noxa-heterozygous parents (in a C57BL/6 background). Figure 7A shows that apoptosis induced by arsenite was almost completely abrogated in Puma-null neurons. However, there was no significant difference between the levels of apoptosis induced in Bim-null, Bim$^{+/-}$, or Bim wt neurons (Fig. 7A), despite the clear differ-

ence in BimEL expression between the three genotypes (a twofold increase in BimEL expression was induced by arsenite in Bim wt neurons, while an increase of about 50% lower intensity was induced in Bim$^{+/-}$ neurons). Moreover, Bim expression was still upregulated 2.3-fold in Puma-null neurons (Fig. 7B), showing that the reason Puma-null neurons were protected was not that Bim was not expressed. P-c-Jun(Ser63) and P-p53(Ser18) were also still upregulated equally in all three Bim genotypes and in Puma-null neurons. There was also no difference in the extent of apoptosis among neurons of the three *Noxa* genotypes (wt, heterozygous, and ko). Although CEP11004 significantly attenuated apoptosis in all sets of wt neurons, it had no significant death-attenuating effects in Puma$^{+/-}$ neurons, a condition where one might have expected it to inhibit the most. However, the reduction from 12.5% ± 2% to 6% ± 0.6% apoptosis in CEP11004-treated Puma$^{-/-}$ neurons, which are wt in Bim, was statistically significant, showing that CEP11004 was still active as an inhibitor of Puma-independent apoptosis.

To confirm that Puma-mediated apoptosis is Bax dependent, as would be expected from the inhibition of arsenite-induced apoptosis in Bax-null neurons, neurons from the progeny of a mating between a Bax$^{+/-}$ male and a Bax-null female were prepared and infected in suspension with 40 PFU per neuron of an Ad construct that expresses human wild-type HA-Puma (Ad-Puma) (116) in conjunction with EGFP expressed under the control of a separate CMV promoter. Apoptosis of neurons that expressed EGFP was analyzed after 20 h, after verification that EGFP-positive neurons were also expressing Puma (Fig. 7D shows that Puma is expressed in punctate cytoplasmic structures). Whereas Ad-Puma promoted a significant amount of apoptosis in the Bax$^{+/-}$ neurons (52% ± 2% [mean ± SD for three animals]), apoptosis was abrogated by 80% in Bax-null neurons (20% ± 3% apoptosis [mean ± SD for four animals], compared to 12% ± 3% apoptosis in uninfected neurons). Levels of apoptosis in wt neurons induced by Ad-EGFP were 10 to 15% (data not shown) (108). In other experiments with wt neurons, apoptosis in response to 40 PFU of Ad-HA-Puma ΔBH3 elicited 20% ± 4% cell death compared to 55% ± 6% cell death with wt Puma (means ± SD from three independent infections), amounts similar to those obtained with HA-Puma in Bax-null and Bax-heterozygous neurons, respectively. Thus, although Puma overexpression induces a powerful apoptotic response in the neurons, this response remains highly Bax dependent.

DISCUSSION

Dominant death insults that overpower the survival mechanisms in neurons may be an underlying cause of several neurodegenerative events. The mechanism by which such signals induce apoptosis is not clear. We have used the pleiotropic compound arsenite, a well-documented environmental CNS toxin (63, 103), to tease out the relationship between dominant death-signaling pathways and activation of BH3-only proteins in cortical neurons. By inducing several death-inducing signals at the same time, we aimed to investigate whether separate streams of signals are allocated to each type of BH3-only protein even when multiple death signals are acting concomitantly, or whether it is the stage of cell death that dictates

BH3-only protein recruitment. We found that arsenite recruited three signals with potential roles in apoptosis: a c-Jun signal that activated Bim expression, a p53 signal that activated Puma (and Noxa) expression, and a reduction in P-Akt, an important antiapoptotic pathway in these neurons (see, for example, references 62, 64, and 66).

To examine which Bcl-2 family members might be affected by these signals, we conducted a comprehensive survey of gene expression. Out of the 19 Bcl-2 family members investigated, we detected 13 different transcripts in 6DIV cultures, expression of some of which has not been described previously. We also noted that some of the transcripts (*Bim*, *Bid*, *Bcl-xL*) were very unstable following treatment with act-D, suggesting that mRNA degradation as well as synthesis regulates steady-state levels of these mRNAs. In human cells a destabilizing response element in the 3′ region of *bcl-2* mRNA has been noted (24), though in the mouse neurons the *bcl-2* transcript appeared to be relatively stable. Under what conditions mRNA degradation is an important putative mode of regulation remains to be determined. Our survey is still incomplete. Clearly all possible Bcl-2 members must be considered in analyzing mechanisms of death in the CNS, especially since it is now clear that some Bcl-2 family members may also play a role in nonapoptotic mechanisms of death that may be more prevalent in disease (92).

Of the six BH3-only members detected, the transcripts of *Puma*, *Bim*, *Bid*, and *Noxa* were increased by treatment with arsenite before cell death began. BimEL, which was the major isoform expressed, and Puma were both increased in the HM fraction during arsenite treatment, alongside an increase in Bax. The location of Puma in the HM fraction is consistent with studies showing that Puma is a mitochondrially targeted protein (70, 115), while the increase in Bim is consistent with its binding to antiapoptotic Bcl-2 family proteins during apoptosis (75). Indeed, 60% of Bcl-xL was initially in the cytosolic fraction, but upon arsenite treatment, all the Bcl-xL was located in the HM fraction (which contained mitochondria and ER), consistent with previous evidence that Bcl-xL is recruited to mitochondria during apoptosis (42). Whether it binds different amounts or types of BH3-only proteins as a result is not clear. We also noted a considerable amount of BimEL present in the HM fraction in unstimulated neurons. This localization is not likely to be due to the presence of microtubules, since no tubulin was detected in the HM fraction. It may be that BimEL is associated with VDAC1/2 at the mitochondria (14, 95) or with antiapoptotic Bcl-2 family members at the ER (reviewed in reference 3) and is thereby prevented from inducing apoptosis constitutively. Alternatively, the multiple bands of BimEL detected on the blots (Fig. 6 and 7) may indicate that it is phosphorylated such that it is prevented from inducing apoptosis (9).

When we analyzed which signals give rise to the upregulation of *Bim*, *Bid*, *Noxa*, and *Puma*, we found that elevation of Bim and Bid expression is dependent on the JNK/c-Jun pathway but not on the p53 pathway, as inhibition of JNK and c-Jun phosphorylation with the MLK inhibitor CEP11004 abrogated the rise in *Bim* and *Bid* mRNA in both wt and p53-null neurons, while their expression was not reduced by a lack of p53. Elevation of BimEL expression was also diminished by CEP11004 or the JNK inhibitor SP600125 but was not altered

by the absence of p53. Inhibition of P-Akt may also have contributed to Bim upregulation, as the PI3-K inhibitor LY294002 inhibited P-Akt while causing a similar increase in BimEL expression (data not shown) (108). By contrast, upregulation of *Puma* and *Noxa* mRNA and of Puma protein was independent of the JNK/c-Jun pathway, as addition of CEP11004 or SP200165 had no effect on their expression. However, the p53 pathway was clearly important in mediating Puma/Noxa expression, as the expression was markedly reduced in neurons from p53-null animals, irrespective of the presence of CEP11004. Nevertheless, a considerable residue of induction remained when both the JNK/c-Jun and p53 pathways were inhibited, suggesting that other pathways that induce Puma and Noxa are activated by arsenite. A p53-independent increase in Noxa mRNA expression (from a lowered basal level) was also noted recently after axotomy of motoneurons in p53$^{-/-}$ mice (54). It is possible that the p53-independent event may be mediated by p63 or p73, important modulators of apoptosis in neurons (46), since both genes can transactivate p53-responsive genes and p73 can both induce Puma (67) and compensate for a lack of p53 (96). In keeping with this idea, we found that induction of the p53-regulated genes *PERP* and *PIDD* was also reduced to about 50% of full expression in p53-null neurons (H. Wong, data not shown). Possible arsenite-dependent, p53-independent pathways include (i) reduced P-Akt, consistent with the results of Han et al., who found that serum deprivation led to a p53-independent increase in Puma/Bbc3 that could be suppressed by IGF-1 in a PI3-K-dependent manner (37); (ii) GADD153/CHOP expression, which was upregulated at the mRNA and protein levels by 100 μM arsenite in cortical neurons (68) and was correlated with increased p53-independent Puma expression in human neuroblastoma cells treated with ER stressors or in rat brain after ischemia (81); (iii) other kinases, in keeping with arsenite-induced phosphorylation of Tau in cortical neurons independent of JNK, ERK, and GSK-3 (33); (iv) elevation of cytoplasmic calcium levels, as arsenite-induced apoptosis of cerebellar granule neurons maintained in 25 mM KCl was blocked by inhibitors of calcium entry (71). Many of these signals may be related to the increased reactive oxygen species induced by arsenite in cortical neurons (E. R. Morrison and A. Wyttenbach, unpublished data). These pathways are currently under investigation.

When we analyzed the extent of apoptosis, it appeared that the JNK/c-Jun pathway and the p53 pathway together accounted for as much as 95% of Bax-dependent apoptosis, since apoptosis was almost completely annulled when p53-null neurons were treated with CEP11004 or SP600125. The possibility that the independence of signaling pathways that induce Puma/Noxa and Bim/Bid is due to P-JNK/c-Jun and p53 operating in separate neuronal populations was dispelled by the finding that the two pathways coexisted in at least 30% of the neurons. Hence, despite several possible cross talk points (see, for example, reference 30), these death signals maintain autonomy down to the particular BH3-only proteins that they employ.

When we studied arsenite-induced apoptosis in neurons from Puma-, Noxa-, or Bim-null mice, a surprising result emerged: Puma was found to be required for >90% of apoptosis, whereas loss of Noxa or Bim conferred no survival advantage. Since the JNK pathway and Bim were still upregulated in the Puma-null neurons, it appears that any apoptotic effects of Bim can be counteracted by resident antiapoptotic mechanisms, including direct inactivation by phosphorylation (9). However, Puma upregulation is not similarly counteracted, making it sufficient to commit the neurons to die. Our data support an essential role for Puma in p53-mediated neuronal death, demonstrated by the substantial decrease found in neuronal death in the developing CNS of γ-irradiated *Puma*-null mice (47) and in p53-treated *Puma*-null cerebellar granule neurons (18). Our findings that transcription and translation, as well as Puma, are required for Bax-mediated apoptosis and that overexpressed Puma cannot induce apoptosis in Bax-null neurons argue against there being a significant direct interaction between p53 and Bax at the mitochondria, recently demonstrated to occur in irradiated mouse brain (26).

Given that we found no reduction in Puma mRNA or protein expression in the presence of CEP11004 in either p53 wt or p53-null neurons, while the CEP11004-sensitive protein BimEL does not mediate arsenite-induced death, why does CEP11004 (and SP600125) still reduce death? One possibility is that JNK contributes to activation of Bax by inducing its translocation to the mitochondria (98). However, in this case, a BH3-only protein is still required for Bax activation at the mitochondria, as Puma-induced death was dependent on Bax and there was little death in the Puma-null neurons. Other possibilities include the contribution of basal JNK activity to death, posttranslational regulation of Puma activity without affecting Puma expression, and/or enhancement of parallel survival pathways that counteract Puma's proapoptotic functions (see, for example, references 37, 84, and 105). The latter notion is supported by our finding that brain-derived neurotrophic factor (BDNF), which prevented the diminution in P-Akt signaling, could also partially postpone Puma-dependent apoptosis (data not shown) (108).

In summary, we have demonstrated a linear relationship between death-signaling pathways and the types of BH3-only proteins that they recruit. It is clear that when a death inducer persists for long periods, it may recruit dormant signals as the cell adjusts to its new signaling environment. If the fixed relationship revealed here between two major death-signaling pathways and the BH3-only proteins they recruit remains constant under other pathological insults, this simplification may have direct bearing on diagnosis and understanding of the disease process. However, it is clear that the impact of each protein on death may depend on factors besides the expression levels per se.

REFERENCES

1. **Akhtar, R. S., J. M. Ness, and K. A. Roth.** 2004. Bcl-2 family regulation of neuronal development and neurodegeneration. Biochim. Biophys. Acta **1644:**189–203.

2. **Anderson, C. N., and A. M. Tolkovsky.** 1999. A role for MAPK/ERK in sympathetic neuron survival: protection against a p53-dependent, JNK-independent induction of apoptosis by cytosine arabinoside. J. Neurosci. **19:**664–673.

3. **Annis, M. G., J. A. Yethon, B. Leber, and D. W. Andrews.** 2004. There is more to life and death than mitochondria: Bcl-2 proteins at the endoplasmic reticulum. Biochim. Biophys. Acta **1644:**115–123.

4. **Antonsson, B., S. Montessuit, S. Lauper, R. Eskes, and J. C. Martinou.** 2000. Bax oligomerization is required for channel-forming activity in liposomes and to trigger cytochrome c release from mitochondria. Biochem. J. **345:**271–278.

5. **Bar-Peled, O., M. Knudson, S. J. Korsmeyer, and J. D. Rothstein.** 1999. Motor neuron degeneration is attenuated in bax-deficient neurons in vitro. J. Neurosci. **55:**542–556.

6. **Bernard, R., S. Dieni, S. Rees, and O. Bernard.** 1998. Physiological and induced neuronal death are not affected in NSE-bax transgenic mice. J. Neurosci. Res. **52:**247–259.

7. **Bhakar, A. L., J. L. Howell, C. E. Paul, A. H. Salehi, E. B. Becker, F. Said, A. Bonni, and P. A. Barker.** 2003. Apoptosis induced by p75NTR overexpression requires Jun kinase-dependent phosphorylation of Bad. J. Neurosci. **23:**11373–11381.

8. **Bhakar, A. L., L. L. Tannis, C. Zeindler, M. P. Russo, C. Jobin, D. S. Park, S. MacPherson, and P. A. Barker.** 2002. Constitutive nuclear factor-κB activity is required for central neuron survival. J. Neurosci. **22:**8466–8475.

9. **Biswas, S. C., and L. A. Greene.** 2002. Nerve growth factor (NGF) down-regulates the Bcl-2 homology 3 (BH3) domain-only protein Bim and suppresses its proapoptotic activity by phosphorylation. J. Biol. Chem. **277:** 49511–49516. (First published 17 October 2002; doi:10.1074/jbc. M208086200.)

10. **Bouillet, P., D. Metcalf, D. C. Huang, D. M. Tarlinton, T. W. Kay, F. Kontgen, J. M. Adams, and A. Strasser.** 1999. Proapoptotic Bcl-2 relative Bim required for certain apoptotic responses, leukocyte homeostasis, and to preclude autoimmunity. Science **286:**1735–1738.

11. **Bouillet, P., and A. Strasser.** 2002. BH3-only proteins—evolutionarily conserved proapoptotic Bcl-2 family members essential for initiating programmed cell death. J. Cell Sci. **115:**1567–1574.

12. **Bushell, M., W. Wood, M. J. Clemens, and S. J. Morley.** 2000. Changes in integrity and association of eukaryotic protein synthesis initiation factors during apoptosis. Eur. J. Biochem. **267:**1083–1091.

13. **Chen, L., S. N. Willis, A. Wei, B. J. Smith, J. I. Fletcher, M. G. Hinds, P. M. Colman, C. L. Day, J. M. Adams, and D. C. Huang.** 2005. Differential targeting of prosurvival Bcl-2 proteins by their BH3-only ligands allows complementary apoptotic function. Mol. Cell **17:**393–403.

14. **Cheng, E. H., T. V. Sheiko, J. K. Fisher, W. J. Craigen, and S. J. Korsmeyer.** 2003. VDAC2 inhibits BAK activation and mitochondrial apoptosis. Science **301:**513–517.

15. **Chittenden, T.** 2002. BH3 domains: intracellular death-ligands critical for initiating apoptosis. Cancer Cell **2:**165–166.

16. **Clarkson, T. W.** 1987. Metal toxicity in the central nervous system. Environ. Health Perspect. **75:**59–64.

17. **Coffey, E. T., G. Smiciene, V. Hongisto, J. Cao, S. Brecht, T. Herdegen, and M. J. Courtney.** 2002. c-Jun N-terminal protein kinase (JNK) 2/3 is specifically activated by stress, mediating c-Jun activation, in the presence of constitutive JNK1 activity in cerebellar neurons. J. Neurosci. **22:**4335–4345.

18. **Cregan, S. P., N. A. Arbour, J. G. MacLaurin, S. M. Callaghan, A. Fortin, E. C. C. Cheung, D. S. Guberman, D. S. Park, and R. S. Slack.** 2004. p53 activation domain 1 is essential for PUMA upregulation and p53-mediated neuronal cell death. J. Neurosci. **24:**10003–10012.

19. **Crowder, R. J., and R. S. Freeman.** 1998. Phosphatidylinositol 3-kinase and Akt protein kinase are necessary and sufficient for the survival of nerve growth factor-dependent sympathetic neurons. J. Neurosci. **18:**2933–2943.

20. **Davies, A. M., and A. Rosenthal.** 1994. Neurons from mouse embryos with a null mutation in the tumour suppressor gene p53 undergo normal cell death in the absence of neurotrophins. Neurosci. Lett. **182:**112–114.

21. **Deckwerth, T. L., J. L. Elliott, C. M. Knudson, E. M. Johnson, Jr., W. D. Snider, and S. J. Korsmeyer.** 1996. BAX is required for neuronal death after trophic factor deprivation and during development. Neuron **17:**401–411.

22. **Degen, W. G., G. J. Pruijn, J. M. Raats, and W. J. van Venrooij.** 2000. Caspase-dependent cleavage of nucleic acids. Cell Death Differ. **7:**616–627.

23. **Domingo, J. L.** 1994. Metal-induced developmental toxicity in mammals: a review. J. Toxicol. Environ. Health **42:**123–141.

24. **Donnini, M., A. Lapucci, L. Papucci, E. Witort, A. Tempestini, G. Brewer, A. Bevilacqua, A. Nicolin, S. Capaccioli, and N. Schiavone.** 2001. Apoptosis is associated with modifications of bcl-2 mRNA AU-binding proteins. Biochem. Biophys. Res. Commun. **287:**1063–1069.

25. **Donovan, N., E. B. Becker, Y. Konishi, and A. Bonni.** 2002. JNK phosphor-

ylation and activation of BAD couples the stress-activated signaling pathway to the cell death machinery. J. Biol. Chem. **277:**40944–40949. (First published 19 August 2002; doi:10.1074/jbc.M206113200.)

26. **Erster, S., M. Mihara, R. H. Kim, O. Petrenko, and U. M. Moll.** 2004. In vivo mitochondrial p53 translocation triggers a rapid first wave of cell death in response to DNA damage that can precede p53 target gene activation. Mol. Cell. Biol. **24:**6728–6741.

27. **Fang, S., J. P. Jensen, R. L. Ludwig, K. H. Vousden, and A. M. Weissman.** 2000. Mdm2 is a RING finger-dependent ubiquitin protein ligase for itself and p53. J. Biol. Chem. **275:**8945–8951.

28. **Filippova, M., and P. J. Duerksen-Hughes.** 2003. Inorganic and dimethylated arsenic species induce cellular p53. Chem. Res. Toxicol. **16:**423–431.

29. **Fu, H. J., Q. S. Hu, Z. N. Lin, T. L. Ren, H. Song, C. K. Cai, and S. Z. Dong.** 2003. Aluminum-induced apoptosis in cultured cortical neurons and its effect on SAPK/JNK signal transduction pathway. Brain Res. **980:**11–23.

30. **Fuchs, S. Y., V. Adler, M. R. Pincus, and Z. Ronai.** 1998. MEKK1/JNK signaling stabilizes and activates p53. Proc. Natl. Acad. Sci. USA **95:**10541–10546.

31. **Garcia-Chavez, E., A. Santamaria, F. Diaz-Barriga, P. Mandeville, B. I. Juarez, and M. E. Jimenez-Capdeville.** 2003. Arsenite-induced formation of hydroxyl radical in the striatum of awake rats. Brain Res. **976:**82–89.

32. **Ghahremani, M. H., E. Keramaris, S. Three, Z. Xia, R. J. Davis, R. Flavell, R. S. Slack, and D. S. Park.** 2002. Interaction of the c-Jun/JNK pathway and cyclin-dependent kinases in death of embryonic cortical neurons evoked by DNA damage. J. Biol. Chem. **277:**35586–35596. (First published 28 June 2002; doi:10.1074/jbc.M204362200.)

33. **Giasson, B. I., D. M. Sampathu, C. A. Wilson, V. Vogelsberg-Ragaglia, W. E. Mushynski, and V. M. Lee.** 2002. The environmental toxin arsenite induces tau hyperphosphorylation. Biochemistry **41:**15376–15387.

34. **Gibson, M. E., B. H. Han, J. Choi, C. M. Knudson, S. J. Korsmeyer, M. Parsadanian, and D. M. Holtzman.** 2001. BAX contributes to apoptotic-like death following neonatal hypoxia-ischemia: evidence for distinct apoptosis pathways. Mol. Med. **7:**644–655.

35. **Gilley, J., P. J. Coffer, and J. Ham.** 2003. FOXO transcription factors directly activate bim gene expression and promote apoptosis in sympathetic neurons. J. Cell Biol. **162:**613–622.

36. **Gross, A., J. M. McDonnell, and S. J. Korsmeyer.** 1999. BCL-2 family members and the mitochondria in apoptosis. Genes Dev. **13:**1899–1911.

37. **Han, J., C. Flemington, A. B. Houghton, Z. Gu, G. P. Zambetti, R. J. Lutz, L. Zhu, and T. Chittenden.** 2001. Expression of bbc3, a pro-apoptotic BH3-only gene, is regulated by diverse cell death and survival signals. Proc. Natl. Acad. Sci. USA **98:**11318–11323.

38. **Harris, C., A. C. Maroney, and E. M. Johnson, Jr.** 2002. Identification of JNK-dependent and -independent components of cerebellar granule neuron apoptosis. J. Neurochem. **83:**992–1001.

39. **Harris, C. A., and E. M. Johnson, Jr.** 2001. BH3-only Bcl-2 family members are coordinately regulated by the JNK pathway and require Bax to induce apoptosis in neurons. J. Biol. Chem. **276:**37754–37760. (First published 8 August 2001; doi:10.1074/jbc.M104073200.)

40. **Haupt, Y., R. Maya, A. Kazaz, and M. Oren.** 1997. Mdm2 promotes the rapid degradation of p53. Nature **387:**296–299.

41. **Hetman, M., K. Kanning, J. E. Cavanaugh, and Z. Xia.** 1999. Neuroprotection by brain-derived neurotrophic factor is mediated by extracellular signal-regulated kinase and phosphatidylinositol 3-kinase. J. Biol. Chem. **274:**22569–22580.

42. **Hsu, Y. T., K. G. Wolter, and R. J. Youle.** 1997. Cytosol-to-membrane redistribution of Bax and Bcl-X(L) during apoptosis. Proc. Natl. Acad. Sci. USA **94:**3668–3672.

43. **Imaizumi, K., A. Benito, S. Kiryu-Seo, V. Gonzalez, N. Inohara, A. P. Leiberman, H. Kiyama, and G. Nunez.** 2004. Critical role for DP5/Harakiri, a Bcl-2 homology domain 3-only Bcl-2 family member, in axotomy-induced neuronal cell death. J. Neurosci. **24:**3721–3725.

44. **Itoh, T., A. Itoh, and D. Pleasure.** 2003. Bcl-2-related protein family gene expression during oligodendroglial differentiation. J. Neurochem. **85:**1500–1512.

45. **Jackson, A. C.** 1999. Apoptosis in experimental rabies in bax-deficient mice. Acta Neuropathol. (Berlin) **98:**288–294.

46. **Jacobs, W. B., G. S. Walsh, and F. D. Miller.** 2004. Neuronal survival and p73/p63/p53: a family affair. Neuroscientist **10:**443–455.

47. **Jeffers, J. R., E. Parganas, Y. Lee, C. Yang, J. Wang, J. Brennan, K. H. MacLean, J. Han, T. Chittenden, J. N. Ihle, P. J. McKinnon, J. L. Cleveland, and G. P. Zambetti.** 2003. Puma is an essential mediator of p53-dependent and -independent apoptotic pathways. Cancer Cell **4:**321–328.

48. **Jeong, S. Y., B. Gaume, Y. J. Lee, Y. T. Hsu, S. W. Ryu, S. H. Yoon, and R. J. Youle.** 2004. Bcl-x(L) sequesters its C-terminal membrane anchor in soluble, cytosolic homodimers. EMBO J. **23:**2146–2155. (First published 6 May 2004; doi:10.1038/sj.emboj.7600225.)

49. **Kapahi, P., T. Takahashi, G. Natoli, S. R. Adams, Y. Chen, R. Y. Tsien, and M. Karin.** 2000. Inhibition of NF-κB activation by arsenite through reaction with a critical cysteine in the activation loop of IκB kinase. J. Biol. Chem. **275:**36062–36066.

50. **Kessis, T. D., R. J. Slebos, W. G. Nelson, M. B. Kastan, B. S. Plunkett, S. M.**

Han, A. T. Lorincz, L. Hedrick, and K. R. Cho. 1993. Human papilloma-virus 16 E6 expression disrupts the p53-mediated cellular response to DNA damage. Proc. Natl. Acad. Sci. USA 90:3988–3992.

51. Kim, A. H., G. Khursigara, X. Sun, T. F. Franke, and M. V. Chao. 2001. Akt phosphorylates and negatively regulates apoptosis signal-regulating kinase 1. Mol. Cell. Biol. 21:893–901.

52. Kim, A. H., H. Yano, H. Cho, D. Meyer, B. Monks, B. Margolis, M. J. Birnbaum, and M. V. Chao. 2002. Akt1 regulates a JNK scaffold during excitotoxic apoptosis. Neuron 35:679–709.

53. Kim, J. Y., H. J. Ahn, J. H. Ryu, K. Suk, and J. H. Park. 2004. BH3-only protein Noxa is a mediator of hypoxic cell death induced by hypoxia-inducible factor 1α. J. Exp. Med. 199:113–124. (First published 29 December 2003; doi:10.1084/jem.20030613.)

54. Kiryu-Seo, S., T. Hirayama, R. Kato, and H. Kiyama. 2005. Noxa is a critical mediator of p53-dependent motor neuron death after nerve injury in adult mouse. J. Neurosci. 25:1442–1447.

55. Klocke, B. J., C. B. Latham, C. D'Sa, and K. A. Roth. 2002. p53 deficiency fails to prevent increased programmed cell death in the Bcl-X(L)-deficient nervous system. Cell Death Differ. 9:1063–1068.

56. Korhonen, L., N. Belluardo, G. Mudo, and D. Lindholm. 2003. Increase in Bcl-2 phosphorylation and reduced levels of BH3-only Bcl-2 family proteins in kainic acid-mediated neuronal death in the rat brain. Eur. J. Neurosci. 18:1121–1134.

57. Krajewska, M., J. K. Mai, J. M. Zapata, K. W. Ashwell, S. L. Schendel, J. C. Reed, and S. Krajewski. 2002. Dynamics of expression of apoptosis-regulatory proteins Bid, Bcl-2, Bcl-X, Bax and Bak during development of murine nervous system. Cell Death Differ. 9:145–157.

58. Kuan, C. Y., K. A. Roth, R. A. Flavell, and P. Rakic. 2000. Mechanisms of programmed cell death in the developing brain. Trends Neurosci. 23:291–297.

59. Kubbutat, M. H., S. N. Jones, and K. H. Vousden. 1997. Regulation of p53 stability by Mdm2. Nature 387:299–303.

60. Kubbutat, M. H., R. L. Ludwig, M. Ashcroft, and K. H. Vousden. 1998. Regulation of Mdm2-directed degradation by the C terminus of p53. Mol. Cell. Biol. 18:5690–5698.

61. Lewis, J., G. A. Oyler, K. Ueno, Y. R. Fannjiang, B. N. Chau, J. Vornov, S. J. Korsmeyer, S. Zou, and J. M. Hardwick. 1999. Inhibition of virus-induced neuronal apoptosis by Bax. Nat. Med. 5:832–835.

62. Liot, G., C. Gabriel, M. Cacquevel, C. Ali, E. T. MacKenzie, A. Buisson, and D. Vivien. 2004. Neurotrophin-3-induced PI-3 kinase/Akt signaling rescues cortical neurons from apoptosis. Exp. Neurol. 187:38–46.

63. Mahata, J., P. Ghosh, J. N. Sarkar, K. Ray, A. T. Natarajan, and A. K. Giri. 2004. Effect of sodium arsenite on peripheral lymphocytes in vitro: individual susceptibility among a population exposed to arsenic through the drinking water. Mutagenesis 19:223–229.

64. Marchetti, L., M. Klein, K. Schlett, K. Pfizenmaier, and U. L. Eisel. 2004. Tumor necrosis factor (TNF)-mediated neuroprotection against glutamate-induced excitotoxicity is enhanced by N-methyl-D-aspartate receptor activation. Essential role of a TNF receptor 2-mediated phosphatidylinositol 3-kinase-dependent NF-κB pathway. J. Biol. Chem. 279:32869–32881. (First published 21 May 2004; doi:10.1074/jbc.M311766200.)

65. Martin, D. P., T. L. Wallace, and E. M. Johnson, Jr. 1990. Cytosine arabinoside kills postmitotic neurons in a fashion resembling trophic factor deprivation: evidence that a deoxycytidine-dependent process may be required for nerve growth factor signal transduction. J. Neurosci. 10:184–193.

66. Matsuzaki, H., K. Namikawa, H. Kiyama, N. Mori, and K. Sato. 2004. Brain-derived neurotrophic factor rescues neuronal death induced by methamphetamine. Biol. Psychiatry 55:52–60.

67. Melino, G., F. Bernassola, M. Ranalli, K. Yee, W. X. Zong, M. Corazzari, R. A. Knight, D. R. Green, C. Thompson, and K. H. Vousden. 2004. p73 induces apoptosis via PUMA transactivation and Bax mitochondrial translocation. J. Biol. Chem. 279:8076–8083. (First published 21 November 2003; doi:10.1074/jbc.M307469200.)

68. Mengesdorf, T., S. Althausen, and W. Paschen. 2002. Genes associated with pro-apoptotic and protective mechanisms are affected differently on exposure of neuronal cell cultures to arsenite. No indication for endoplasmic reticulum stress despite activation of grp78 and gadd153 expression. Brain Res. Mol. Brain Res. 104:227–239.

69. Murakata, C., M. Kaneko, G. Gessner, T. S. Angeles, M. A. Ator, T. M. O'Kane, B. A. McKenna, B. A. Thomas, J. R. Mathiasen, M. S. Saporito, D. Bozyczko-Coyne, and R. L. Hudkins. 2002. Mixed lineage kinase activity of indolocarbazole analogues. Bioorg. Med. Chem. Lett. 12:147–150.

70. Nakano, K., and K. H. Vousden. 2001. PUMA, a novel proapoptotic gene, is induced by p53. Mol. Cell 7:683–694.

71. Namgung, U., D. H. Kim, S. R. Lim, and Z. Xia. 2003. Blockade of calcium entry accelerates arsenite-mediated apoptosis in rat cerebellar granule cells. Mol. Cells 15:256–261.

72. Namgung, U., and Z. Xia. 2001. Arsenic induces apoptosis in rat cerebellar neurons via activation of JNK3 and p38 MAP kinases. Toxicol. Appl. Pharmacol. 174:130–138.

73. Namgung, U., and Z. Xia. 2000. Arsenite-induced apoptosis in cortical

74. Napankangas, U., N. Lindqvist, D. Lindholm, and F. Hallbook. 2003. Rat retinal ganglion cells upregulate the pro-apoptotic BH3-only protein Bim after optic nerve transection. Brain Res. Mol. Brain Res. 120:30–37.

75. O'Connor, L., A. Strasser, L. A. O'Reilly, G. Hausmann, J. M. Adams, S. Cory, and D. C. Huang. 1998. Bim: a novel member of the Bcl-2 family that promotes apoptosis. EMBO J. 17:384–395.

76. Park, D. S., E. J. Morris, L. Stefanis, C. M. Troy, M. L. Shelanski, H. M. Geller, and L. A. Greene. 1998. Multiple pathways of neuronal death induced by DNA-damaging agents, NGF deprivation, and oxidative stress. J. Neurosci. 18:830–840.

77. Polster, B. M., K. W. Kinnally, and G. Fiskum. 2001. BH3 death domain peptide induces cell type-selective mitochondrial outer membrane permeability. J. Biol. Chem. 276:37887–37894.

78. Putcha, G. V., K. L. Moulder, J. P. Golden, P. Bouillet, J. A. Adams, A. Strasser, and E. M. Johnson. 2001. Induction of BIM, a proapoptotic BH3-only BCL-2 family member, is critical for neuronal apoptosis. Neuron 29:615–628.

79. Puthalakath, H., and A. Strasser. 2002. Keeping killers on a tight leash: transcriptional and post-translational control of the pro-apoptotic activity of BH3-only proteins. Cell Death Differ. 9:505–512.

80. Puthalakath, H., A. Villunger, L. A. O'Reilly, J. G. Beaumont, L. Coultas, R. E. Cheney, D. C. Huang, and A. Strasser. 2001. Bmf: a proapoptotic BH3-only protein regulated by interaction with the myosin V actin motor complex, activated by anoikis. Science 293:1829–1832.

81. Reimertz, C., D. Kogel, A. Rami, T. Chittenden, and J. H. Prehn. 2003. Gene expression during ER stress-induced apoptosis in neurons: induction of the BH3-only protein Bbc3/PUMA and activation of the mitochondrial apoptosis pathway. J. Cell Biol. 162:587–597.

82. Rideout, H. J., E. Zang, M. Yeasmin, R. Gordon, O. Jabado, D. S. Park, and L. Stefanis. 2001. Inhibitors of trypsin-like serine proteases prevent DNA damage-induced neuronal death by acting upstream of the mitochondrial checkpoint and of p53 induction. Neuroscience 107:339–352.

83. Rodriguez, V. M., L. Carrizales, M. E. Jimenez-Capdeville, L. Dufour, and M. Giordano. 2001. The effects of sodium arsenite exposure on behavioral parameters in the rat. Brain Res. Bull. 55:301–308.

84. Roux, P. P., G. Dorval, M. Boudreau, A. Angers-Loustau, S. J. Morris, J. Makkerh, and P. A. Barker. 2002. K252a and CEP1347 are neuroprotective compounds that inhibit mixed-lineage kinase-3 and induce activation of Akt and ERK. J. Biol. Chem. 277:49473–49480. (First published 17 October 2002; doi:10.1074/jbc.M203428200.)

85. Salazar, A. M., P. Ostrosky-Wegman, D. Menendez, E. Miranda, A. Garcia-Carranca, and E. Rojas. 1997. Induction of p53 protein expression by sodium arsenite. Mutat. Res. 381:259–265.

86. Samuel, S., R. Kathirvel, T. Jayavelu, and P. Chinnakkannu. 2005. Protein oxidative damage in arsenic induced rat brain: influence of DL-alpha-lipoic acid. Toxicol. Lett. 155:27–34.

87. Scorrano, L., and S. J. Korsmeyer. 2003. Mechanisms of cytochrome c release by proapoptotic BCL-2 family members. Biochem. Biophys. Res. Commun. 304:437–444.

88. Selimi, F., M. W. Vogel, and J. Mariani. 2000. Bax inactivation in lurcher mutants rescues cerebellar granule cells but not purkinje cells or inferior olivary neurons. J. Neurosci. 20:5339–5345.

89. Shalat, S. L., D. B. Walker, and R. H. Finnell. 1996. Role of arsenic as a reproductive toxin with particular attention to neural tube defects. J. Toxicol. Environ. Health 48:253–272.

90. Shi, L., S. Gong, Z. Yuan, C. Ma, Y. Liu, C. Wang, W. Li, R. Pi, S. Huang, R. Chen, Y. Han, Z. Mao, and M. Li. 2005. Activity deprivation-dependent induction of the proapoptotic BH3-only protein Bim is independent of JNK/c-Jun activation during apoptosis in cerebellar granule neurons. Neurosci. Lett. 375:7–12. (First published 24 November 2004; doi:10.1016/j.neulet.2004.10.082.).

91. Shibata, M., H. Hattori, T. Sasaki, J. Gotoh, J. Hamada, and Y. Fukuuchi. 2002. Temporal profiles of the subcellular localization of Bim, a BH3-only protein, during middle cerebral artery occlusion in mice. J. Cereb. Blood Flow Metab. 22:810–820.

92. Shimizu, S., T. Kanaseki, N. Mizushima, T. Mizuta, S. Arakawa-Kobayashi, C. B. Thompson, and Y. Tsujimoto. 2004. Role of Bcl-2 family proteins in a non-apoptotic programmed cell death dependent on autophagy genes. Nat. Cell Biol. 6:1221–1228.

93. Shindler, K. S., C. B. Latham, and K. A. Roth. 1997. Bax deficiency prevents the increased cell death of immature neurons in bcl-x-deficient mice. J. Neurosci. 17:3112–3119.

94. Shinoda, S., C. K. Schindler, J. Quan-Lan, J. A. Saugstad, W. Taki, R. P. Simon, and D. C. Henshall. 2003. Interaction of 14-3-3 with Bid during seizure-induced neuronal death. J. Neurochem. 86:460–469.

95. Sugiyama, T., S. Shimizu, Y. Matsuoka, Y. Yoneda, and Y. Tsujimoto. 2002. Activation of mitochondrial voltage-dependent anion channel by a proapoptotic BH3-only protein Bim. Oncogene 21:4944–4956.

96. Suliman, Y., O. G. Opitz, A. Avadhani, T. C. Burns, W. El-Deiry, D. T.

Wong, and A. K. Rustgi. 2001. p63 expression is associated with p53 loss in oral-esophageal epithelia of p53-deficient mice. Cancer Res. **61:**6467–6473.

97. **Tomkins, C. E., S. N. Edwards, and A. M. Tolkovsky.** 1994. Apoptosis is induced in post-mitotic rat sympathetic neurons by arabinosides and topo-isomerase II inhibitors in the presence of NGF. J. Cell Sci. **107:**1499–1507.

98. **Tsuruta, F., J. Sunayama, Y. Mori, S. Hattori, S. Shimizu, Y. Tsujimoto, K. Yoshioka, N. Masuyama, and Y. Gotoh.** 2004. JNK promotes Bax translo-cation to mitochondria through phosphorylation of 14-3-3 proteins. EMBO J. **23:**1889–1899.

99. **Uo, T., Y. Kinoshita, and R. S. Morrison.** 2005. Neurons exclusively express N-Bak, a BH3 domain-only Bak isoform that promotes neuronal apoptosis. J. Biol. Chem. **280:**9065–9073. (First published 8 December 2004; doi: 10.1074/jbc.M413030200.)

100. **Villunger, A., E. M. Michalak, L. Coultas, F. Mullauer, G. Bock, M. J. Ausserlechner, J. M. Adams, and A. Strasser.** 2003. p53- and drug-induced apoptotic responses mediated by BH3-only proteins Puma and Noxa. Sci-ence **302:**1036–1038.

101. **Virdee, K., A. J. Bannister, S. P. Hunt, and A. M. Tolkovsky.** 1997. Com-parison between the timing of JNK activation, c-Jun phosphorylation, and onset of death commitment in sympathetic neurones. J. Neurochem. **69:** 550–561.

102. **Virdee, K., L. Xue, B. A. Hemmings, C. Goemans, R. Heumann, and A. M. Tolkovsky.** 1999. Nerve growth factor-induced PKB/Akt activity is sustained by phosphoinositide 3-kinase dependent and independent signals in sym-pathetic neurons. Brain Res. **837:**127–142.

103. **Waalkes, M. P., J. Liu, J. M. Ward, and B. A. Diwan.** 2004. Mechanisms underlying arsenic carcinogenesis: hypersensitivity of mice exposed to in-organic arsenic during gestation. Toxicology **198:**31–38.

104. **Wakabayashi, T., J. Kosaka, and S. Hommura.** 2002. Up-regulation of Hrk, a regulator of cell death, in retinal ganglion cells of axotomized rat retina. Neurosci. Lett. **318:**77–80.

105. **Wang, L. H., A. J. Paden, and E. M. Johnson, Jr.** 2005. Mixed-lineage kinase inhibitors require the activation of Trk receptors to maintain long-term neuronal trophism and survival. J. Pharmacol. Exp. Ther. **312:**1007–1019. (First published 3 November 2004; doi:10.1124/jpet.104.077800.)

106. **White, F. A., C. R. Keller-Peck, C. M. Knudson, S. J. Korsmeyer, and W. D. Snider.** 1998. Widespread elimination of naturally occurring neuronal death in Bax-deficient mice. J. Neurosci. **18:**1428–1439.

107. **Whitfield, J., S. J. Neame, L. Paquet, O. Bernard, and J. Ham.** 2001. Dominant-negative c-Jun promotes neuronal survival by reducing BIM expression and inhibiting mitochondrial cytochrome *c* release. Neuron **29:** 629–643.

108. **Wong, H. K.** 2004. Ph.D. thesis. University of Cambridge, Cambridge, United Kingdom.

109. **Xiang, H., D. W. Hochman, H. Saya, T. Fujiwara, P. A. Schwartzkroin, and R. S. Morrison.** 1996. Evidence for p53-mediated modulation of neuronal viability. J. Neurosci. **16:**6753–6765.

110. **Xiang, H., Y. Kinoshita, C. M. Knudson, S. J. Korsmeyer, P. A. Schwartz-kroin, and R. S. Morrison.** 1998. Bax involvement in p53-mediated neuro-nal cell death. J. Neurosci. **18:**1363–1373.

111. **Xu, X., J. Raber, D. Yang, B. Su, and L. Mucke.** 1997. Dynamic regulation of c-Jun N-terminal kinase activity in mouse brain by environmental stimuli. Proc. Natl. Acad. Sci. USA **94:**12655–12660.

112. **Xue, L., J. H. Murray, and A. M. Tolkovsky.** 2000. The Ras/phosphatidyl-inositol 3-kinase and Ras/ERK pathways function as independent survival modules each of which inhibits a distinct apoptotic signaling pathway in sympathetic neurons. J. Biol. Chem. **275:**8817–8824.

113. **Yih, L. H., and T. C. Lee.** 2000. Arsenite induces p53 accumulation through an ATM-dependent pathway in human fibroblasts. Cancer Res. **60:**6346–6352.

114. **Yin, X. M., Y. Luo, G. Cao, L. Bai, W. Pei, D. K. Kuharsky, and J. Chen.** 2002. Bid-mediated mitochondrial pathway is critical to ischemic neuronal apoptosis and focal cerebral ischemia. J. Biol. Chem. **277:**42074–42081. (First published 27 August 2002; doi:10.1074/jbc.M204991200.)

115. **Yu, J., Z. Wang, K. W. Kinzler, B. Vogelstein, and L. Zhang.** 2003. PUMA mediates the apoptotic response to p53 in colorectal cancer cells. Proc. Natl. Acad. Sci. USA **100:**1931–1936.

116. **Yu, J., L. Zhang, P. M. Hwang, K. W. Kinzler, and B. Vogelstein.** 2001. Puma induces the rapid apoptosis of colorectal cancer cells. Mol. Cell **7:**673–682.